

In Revision

microRNA-124 regulates *Notch* and *NeuroD1* to mediate transition states of neuronal development

Running title: miR-124 suppresses *Notch* and *NeuroD1*

Kalin D. Konrad¹ and Jia L. Song^{1*}

¹Department of Biological Sciences, University of Delaware, Newark, DE 19711, USA

* Corresponding author/lead contact, email: jsong@udel.edu

Author contributions

K.D.K. and J.L.S. conceived the experiments and wrote the paper. K.D.K. performed and analyzed all the experiments.

Acknowledgments

We thank Dr. Gary Wessel (Brown University) for the Endo1 and SynB antibodies. We thank members of our laboratory for their comments. We also thank the anonymous reviewers for their valuable feedback.

Funding

This work is funded by National Science Foundation (IOS 1553338 and MCB 2103453 to J.L.S.), NIH P20GM103653, NIH NIGMS P20GM103446, and Sigma Xi Grants-in-Aid of Research (G2018031596227966 to K.D.K.).

Data Sharing and Data Accessibility

The data that support the findings of this study are available from the corresponding author upon reasonable request.

Conflict of Interest

This article has been accepted for publication and undergone full peer review but has not been through the copyediting, typesetting, pagination and proofreading process, which may lead to differences between this version and the [Version of Record](https://doi.org/10.1002/dneu.22902). Please cite this article as [doi: 10.1002/dneu.22902](https://doi.org/10.1002/dneu.22902).

This article is protected by copyright. All rights reserved.

The authors declare no competing or financial interests.

Abstract

MicroRNAs regulate gene expression by destabilizing target mRNA and/or inhibiting translation in animal cells. The ability to mechanistically dissect miR-124's function during specification, differentiation, and maturation of neurons during development within a single system has not been accomplished. Using the sea urchin embryo, we take advantage of the manipulability of the embryo and its well-documented gene regulatory networks (GRNs). We incorporated *NeuroD1* as part of the sea urchin neuronal GRN and determined that miR-124 inhibition resulted in aberrant gut contractions, swimming velocity, and neuronal development. Inhibition of miR-124 resulted in an increased number of cells expressing transcription factors associated with progenitor neurons and a concurrent decrease of mature and functional neurons. Results revealed that in the early blastula/gastrula stages, miR-124 regulates undefined factors during neuronal specification and differentiation. In the late gastrula/larval stages, miR-124 regulates *Notch* and *NeuroD1* during the transition between neuronal differentiation and maturation. Overall, we have improved the neuronal GRN and identified miR-124 to play a prolific role in regulating various transitions of neuronal development.

Key words: sea urchin, post-transcriptional regulation, gene regulatory network, neurogenesis, signaling pathways.

Introduction

Although the body plan and neuronal organization of deuterostomes are diverse, developmental mechanisms that mediate the specification and differentiation of their nervous systems share striking similarities at the molecular level. It has been observed that sea urchin neuronal-specific *Pou4f2* (*Brn*) can functionally replace *Pou4f2* in mice, revealing a strong level of conservation in neuronal development across the species (Mao et al., 2016). Both vertebrate and sea urchin embryos use the FGF signaling pathway to initiate neurogenesis (Garner et al., 2016; Kengaku & Okamoto, 1993; Rentzsch, Fritzenwanker, Scholz, &

Technau, 2008), Nodal and BMP pathways to restrict dorsal-ventral neuronal regions (Litsiou, Hanson, & Streit, 2005; S. Yaguchi, Yaguchi, & Burke, 2006), Wnt signaling to suppress neuronal development (Braun, Etheridge, Bernard, Robertson, & Roelink, 2003; Range, 2018), and the Delta/Notch pathway to mediate classical lateral inhibition, resulting in *Delta*-expressing differentiated neurons (Mellott, Thisdelle, & Burke, 2017; Siebel & Lendahl, 2017). Additionally, Sox transcription factors (TFs), NeuroD, Pou/Brn, and Elav are all conserved proteins driving specification, differentiation, and maturation of neurons, respectively (Mao et al., 2016; McClay, Miranda, & Feinberg, 2018; Perillo et al., 2018; Zaharieva, Haussmann, Brauer, & Soller, 2015). Thus, the sea urchin embryo uses evolutionarily conserved TFs and signaling pathways to set up the nervous system.

Out of all the conserved proteins, none of the family member of NeuroD have been incorporated into the sea urchin neuronal gene regulatory network (GRN). NeuroD (NeuroD1, NeuroD2, and NeuroD6) TFs are members of the neuronal lineage basic helix-loop-helix family that regulate the transition from neuronal differentiation to maturation in vertebrate/invertebrate systems (Amador-Arjona et al., 2015; Aquino-Nunez et al., 2020; Cho & Tsai, 2004; Huang et al., 2011; Liu et al., 2011; Masoudi et al., 2018; Matsuda et al., 2019; Pataskar et al., 2016). NeuroD1, specifically, is expressed early in mammalian embryos to regulate neuronal development, suggesting that it is a good candidate to be incorporated into the sea urchin neuronal GRN (Matsuda et al., 2019; Pataskar et al., 2016; Tutukova, Tarabykin, & Hernandez-Miranda, 2021). We aim to make a more comprehensive gene regulatory network (GRN) by incorporating the function of NeuroD1 into the network.

The nervous system in the sea urchin larva contains three neuronal centers: the apical organ and ganglionic organization analogous to the vertebrate central nervous system; the ciliary band that coordinates larval swimming, analogous to the peripheral nervous system; and enteric neurons that mediate gut contractions (Fig. 1A) (Krupke & Burke, 2014; Otim, Amore, Minokawa, McClay, & Davidson, 2004). Initiation of specification starts early in development, where SoxB1 activates *Foxq2* and *SoxC* which are both TFs expressed in the apical domain (McClay et al., 2018). The expression of *Foxq2* in the anterior neuroectoderm is restricted by canonical Wnt signaling pathway (*Wnt6*) early in blastula and is critical in proper development

of serotonergic neurons (L. M. Angerer, Yaguchi, Angerer, & Burke, 2011; McClay et al., 2018; J. Yaguchi, Takeda, Inaba, & Yaguchi, 2016; S. Yaguchi, Yaguchi, Angerer, & Angerer, 2008). Once the neuronal *SoxC*-positive progenitors undergo their last mitotic division, the two daughter cells contain varying levels of Delta and Notch proteins (Garner et al., 2016; Mellott et al., 2017). There will be some cells during the late gastrula to the early larval stage where *Delta* will co-express with *Brn1/2/4*, while the other daughter cell with more Notch undergoes apoptosis (Garner et al., 2016; Mellott et al., 2017; Torii, 2012; Truman, Moats, Altman, Marin, & Williams, 2010). The mechanism that activates Notch signaling in the non-neuronal cell is unclear (Mellott et al., 2017). During the larval stage, the neurons will eventually stop expressing *Delta* as the differentiated neuron becomes a mature/functional neuron (Garner et al., 2016; Mellott et al., 2017; Torii, 2012; Truman et al., 2010). Thus, there will be some neurons that initially co-express *Delta* and *Brn1/2/4*, then as differentiation proceeds, the neurons will only express *Brn1/2/4*. Differentiated, mature neurons in the ciliary band and apical organ express *Elav* (Garner et al., 2016), which is an RNA binding protein that stabilizes transcripts regulating axonal guidance and synaptic growth (Wang et al., 2015; Zaharieva et al., 2015). The mature and functional neurons will also express Synaptotagmin B (SynB), which is part of the SNARE family mediating synaptic release of neurotransmitters (Burke et al., 2006; DeBello, Betz, & Augustine, 1993). Serotonergic neurons in the neuroectoderm also express serotonin which is a neurotransmitter important for mediating larval gut contractions, early swimming, and feeding behavior (Zheng Wei, Angerer, & Angerer, 2016; S. Yaguchi & Katow, 2003).

The monociliated epithelial cells that reside in the ciliary band (Krupke & Burke, 2014) are formed from a ventral-dorsal boundary where Nodal and BMP2/4 signaling pathways are inactive. *Onecut (Hnf6)* is expressed in the ciliary band where it enables the formation of neuronal connections and it is expressed juxtaposed to where neurons reside (Otim et al., 2004; van der Raadt, van Gestel, Nadif Kasri, & Albers, 2019). In other systems, *Onecut* is important for neuronal differentiation as well as in promoting neuromuscular junctions (Audouard et al., 2012; Toch et al., 2020).

The third domain of neurons resides in the tripartite gut to mediate muscular contractions for feeding (Fig. 1A) (Z. Wei, Angerer, & Angerer, 2011). The

compartments of the gut are separated by mesodermally-derived sphincters: the cardiac sphincter separates the foregut and the midgut; the pyloric sphincter separates the midgut and the hindgut and the anal sphincter at the blastopore (Wessel & Wikramanayake, 1999). The neurons that reside in the mid/foregut are endodermally-derived (Z. Wei et al., 2011). Less is known about the enteric neurons; however, *SoxB1*, *SoxC*, *Six3*, *Delta*, and *Nkx2-3* expression in the endomesoderm could specify the neuroendoderm but remains unclear (McClay et al., 2018; Z. Wei et al., 2011). Recently, it has been shown that the opening of the pyloric sphincter is responsive to light, resulting from released serotonin that binds to receptors in the midgut to mediate contraction (Junko Yaguchi & Yaguchi, 2021). During the larval stage, in response to calcium influx and release of different neurotransmitters, neurons in these three neuronal domains mediate swimming and feeding behavior (Kato, Yaguchi, & Kyoizuka, 2007).

From vertebrates to invertebrates, miR-124 is expressed in neuronal tissues and plays an evolutionarily conserved function in regulating the balance between neuronal cell proliferation and differentiation (Chen, Pedro, & Zeller, 2011; Makeyev, Zhang, Carrasco, & Maniatis, 2007; Rajasethupathy et al., 2009; Weng & Cohen, 2012). miR-124 regulates *SRY-transcription factor*, *Polypyrimidine Tract-Binding Protein 1*, *Notch*, and *NeuroD1*, to name a few; human miR-124-1 deletions have been shown to be associated with psychiatric disorders, and mice with miR-124-1 deficiency resulted in central nervous system abnormalities (Ambasudhan et al., 2011; Chen et al., 2011; Kozuka et al., 2019; Liu et al., 2011; Makeyev et al., 2007). Although the function of miR-124 has been examined previously (Liu et al., 2011; Weng & Cohen, 2012; Yu, Chung, Deo, Thompson, & Turner, 2008), a systematic and comprehensive understanding of miR-124's role in neuronal specification, differentiation, and maturation in a developing embryo is still lacking. The sea urchin embryo serves as a powerful model to integrate post-transcriptional regulation of neurogenesis, because neurogenesis can be closely followed throughout development (L. M. Angerer et al., 2011; Garner et al., 2016). Additionally, the sea urchin embryo contains ~50 miRNAs compared to the ~500 miRNAs identified in humans and mice (Bartel, 2009, 2018; Lewis, Burge, & Bartel, 2005). With a single sea urchin miR-124, compared to the three different copies in the mouse, the sea urchin embryo is a tractable model to examine its function (Kozuka et al., 2019; Song

et al., 2012). Additionally, the ability to test the impact of selectively blocking miR-124's suppression of its specific targets enables us to dissect miR-124's role in neuronal development (Remsburg, Konrad, Sampilo, & Song, 2019).

The purple sea urchin has one of the most comprehensive gene regulatory networks (GRN), but the neuronal GRN is less defined. In the current study, we first sought to construct a more complete neuronal GRN by incorporating the function of NeuroD1 into the existing neuronal GRN, since it is a well-known transcription factor involved in vertebrate neurogenesis (Puligilla, Dabdoub, Brenowitz, & Kelley, 2010; Tutukova et al., 2021). Results indicate that perturbation of the sea urchin NeuroD1 leads to expression changes of *SoxC*, *Delta*, *Brn1/2/4*, and *Elav*. With this updated network, our goal is to discover miR-124's post-transcriptional regulation within the neuronal GRN. First, we examined how miR-124 post-transcriptionally regulates development at the whole embryo level, with the focus on neural development. We dissected miR-124's regulatory role during neurogenesis, by using neuronal progenitor markers to follow the specification (*Foxq2*), differentiation (*SoxC*, *Brn1/2/4*, *NeuroD1*), maturation of neurons (*Elav*), and functional neurons (*SynB*) to examine the impact of miR-124's regulatory role at each of these stages. Results indicate that inhibition of miR-124 results in an increased number of cells expressing TFs associated with progenitor neurons, such as *FoxQ2*, *SoxC*, and *Brn1/2/4*, and a concomitant decrease of serotonin-expressing neurons and *SynB*-positive functional neurons. Then, we used bioinformatics and reporter constructs and identified that miR-124 directly suppresses *Notch* and *NeuroD1*. We examined the impact of blocking miR-124's suppression of *NeuroD1* and found this regulation to be important for differentiation of neurons. Furthermore, we found that miR-124's suppression of *Notch* and *NeuroD1* phenocopies miR-124 inhibitor-induced defects, indicating that miR-124 fine-tunes these factors to control neuronal development. Overall, we integrate NeuroD1 into the sea urchin neuronal GRN and systematically define miR-124's regulatory role throughout neurogenesis by identifying its regulatory role within the neuronal GRN.

Materials and methods

Animals

Adult *Strongylocentrotus purpuratus* were collected from the California coast (Pt. Loma Marine Invertebrate Lab or Marinus Scientific, LLC.). All animals and cultures were incubated at 15°C.

Real-time, quantitative polymerase chain reaction (qPCR)

To assess the relative quantity of *NeuroD1* transcripts throughout development, we collected 200 embryos at different development stages and extracted total RNA with an RNA XS kit (Macherey-Nagel, Allentown, PA). For *NeuroD1* MASO, miR-124 inhibitor, and *NeuroD1* morpholino-based target protector (TP) -injected embryos (Remsburg et al., 2019; Staton & Giraldez, 2011), 100 embryos were collected, and RNA extracted. cDNA was synthesized using the iScript cDNA Synthesis Kit (Bio-Rad, Philadelphia, PA). qPCR was performed using two embryo-equivalents for each reaction using Power SYBR Green PCR Master Mix (Invitrogen, Waltham, MA) in the Quantstudio6 Real-time PCR machine (Applied Biosystems, Waltham, MA) as previously described (N. A. Stepicheva & Song, 2015). Primers were designed using the Primer3 program (Table 1) (Rozen & Skaletsky, 2000) (Primer3, RRID:SCR_003139).

Microinjections

Microinjections were performed as previously described with modifications (N. A. Stepicheva & Song, 2014). *Hsa-miR-124-3p* Locked Nucleic Acid (LNA) power inhibitor and *Hsa-miR-124-3p* miRCURY LNA miRNA mimic (Qiagen, Germantown, MD) were resuspended with RNase-free water to 100 µM. All sequences are listed in Table 1. Embryos were injected with the different concentrations (10 µM, 15 µM, and 20 µM) of miR-124 LNA inhibitor and collected at gastrula stage to phenotype for developmental defects. Based on the dose-response results, we used 15 µM of the *Hsa-miR-124-3p* LNA power inhibitor for subsequent experiments. The *Hsa-miR-124-3p* miRCURY LNA miRNA mimic (Qiagen, Germantown, MD) was used at 15 µM with miR-124 inhibitor. To block miR-124's binding and regulation of *NeuroD1*, we designed a *NeuroD1* TP MASO against the miR-124 binding site within *NeuroD1*'s coding sequence (CDS) (GeneTools, LLC, Philomath, OR) (Remsburg et al., 2019). *NeuroD1* TP and control MASO (human *beta-globin*) was resuspended to a 5 mM stock solution with RNase-free water and diluted to 15 µM, 30 µM, and 300 µM to perform microinjections. Zygotes were injected with different concentrations of TPs and were phenotyped for defects. Based on the dose-response results of

NeuroD1 TP experiments, we used 30 μ M of TPs for subsequent experiments. For negative controls, we used the negative control against the human β -globin gene. In addition, we designed two *Control Notch* TPs and two *Control NeuroD1* TPs against different regions of the transcripts that did not contain the validated miR-124 binding sites. We injected *Notch* and/or *NeuroD1* wildtype luciferase construct with either of these three negative controls or *Notch* TP and *NeuroD1* TP that specifically block the validated miR-124 binding sites. Translational blocking MASO against *NeuroD1* (GeneTools, LLC, Philomath, OR) was resuspended to a 5 mM stock solution with RNase-free water and diluted to 6 μ M, 30 μ M, and 150 μ M to perform loss-of-function studies. Based on the dose-response results, we used 30 μ M of the *NeuroD1* MASO, where we observed ~50% of injected blastulae survived, for subsequent experiments (Sequences of TPs and MASOs are listed in Table 1).

Injection solutions contained 20% sterile glycerol, 2 mg/mL 10,000 MW Texas Red or FITC lysine charged dextran (ThermoFisher Scientific, Waltham, MA), and various concentrations of miR-124 inhibitor, miR-124 mimic, *NeuroD1* translational blocking MASO, *Notch* TP, *NeuroD1* TP, or Control TPs. Injections were performed using the Pneumatic PicoPump with a vacuum (World Precision Instruments; Sarasota, FL). A vertical needle puller PL-10 (Narishige International, USA, INC., Amityville, NY) was used to pull the injection needles (1 mm glass capillaries with filaments) (Narishige International, USA, INC., Amityville, NY).

RNA *in situ* hybridization

The steps performed for fluorescence RNA *in situ* hybridization (FISH) are described previously with modifications (Sethi, Angerer, & Angerer, 2014). All sequences are listed in Table 1. The *Hsa*-miR-124-3p miRCURY LNA detection probe (Qiagen, Germantown, MD) was used to visualize sea urchin miR-124 (at 0.5 ng/ μ L) in hybridization buffer and incubated at 50°C for five days. The scrambled-miR miRCURY LNA detection probe was used as a negative control (Qiagen, Germantown, MD, cat# YD00699004) at the same concentration as miR-124 probe.

To generate RNA probes against protein-coding transcripts, we used PCR to amplify *SoxB1*, *Foxq2*, *Onecut (Hnf6)*, *SoxC*, *Brn1/2/4*, *Elav*, and *Delta* from sea urchin egg and embryonic cDNA of 24 hpf, 48 hpf, 72 hpf. PCR primers and enzymes used to linearize and make antisense probes are listed in Table 1 (SpBase - *Strongylocentrotus purpuratus*: the Sea Urchin Genome Database,

RRID:SCR_007441). Other probes including *FoxA*, *Krl*, and *Vasa* were previously cloned (N. Stepicheva, Nigam, Siddam, Peng, & Song, 2015). 0.5 µg probe/mL was used to detect native transcript in embryos, according to previous protocols (N. A. Stepicheva & Song, 2015).

For double FISH, we incubated *Onecut* (fluorescein-labeled) with miR-124 (DIG-labeled) together. The scrambled miR miRCURY LNA detection probe was used as a negative control with miR-124 FISH. The negative control for the fluorescein-labeled probe was from the control DNA 1 plasmid, pSPT18-Neo construct included in the RNA DIG labeling kit (MilliporeSigma, St. Louis, MO), using the fluorescein RNA labeling mix (MilliporeSigma, St. Louis, MO). All probes were added at 0.5 ng/µL. We incubated embryos with the anti-fluorescein-HRP antibody first overnight at 1:250 concentration at RT and labeled them with fluorescein-tyramide using tyramide signal amplification (TSA). Then we quenched the reaction with 3% hydrogen peroxide in MOPS buffer for 1 h at RT. Then we incubated embryos with DIG antibody at 1:1,000 concentration overnight at 4°C and labeled them with Cy5.5 tyramide using TSA (Akoya Biosciences, Marlborough, MA). For single FISH, we incubated the embryos with the 1:1,000 anti-digoxigenin (DIG)-POD antibody overnight at 4°C and amplified with Tyramide Amplification working solution and exposed with fluorescein (1:150 dilution of TSA stock with 1x Plus Amplification Diluent-fluorescein) (Akoya Biosciences, Marlborough, MA).

For FISH all the probes were added at 0.5 ng/µL. All FISH embryos were mounted in MOPS buffer and NucBlue (Thermo Fisher Scientific, Waltham, MA). Images were taken using the Zeiss LSM 880 scanning confocal microscope (Carl Zeiss Incorporation, White Plains, NY) (Zeiss LSM 880 with Airyscan Confocal Laser Scanning Microscope (RRID:SCR_020925)). The maximum intensity projections of Z-stack images were acquired with Zen software and processed with Adobe Photoshop (RRID:SCR_014199) and Adobe Illustrator (Adobe, San Jose, CA) (RRID:SCR_010279).

The steps performed for colorimetric whole-mount *in situ* hybridization (WMISH) are as previously described (Arenas-Mena, Cameron, & Davidson, 2000; Minokawa, Rast, Arenas-Mena, Franco, & Davidson, 2004). Negative controls were transcribed off plasmid pSPT18-Neo or pSPT19-Neo provided in the DIG RNA Labeling kit (MilliporeSigma, St. Louis, MO). All probes were added at 0.5 ng/µL.

Embryos were incubated at 1:1500 anti-digoxigenin-alkaline phosphatase antibody overnight at RT. Embryos were imaged using the Observer Z.1 microscope (Carl Zeiss Incorporation, White Plains, NY) (Zeiss Axio Observer (RRID:SCR_021351)). The Z-stack slice at the equatorial plane was taken and processed with Adobe Photoshop (RRID:SCR_014199) and Adobe Illustrator (Adobe, San Jose, CA) (RRID:SCR_010279).

Immunolabeling procedures

To assess miR-124 inhibitor-induced phenotypes, we used antibodies against various cell types. We used Endo1 to detect mid- and hindgut (Wessel & McClay, 1985), E7 (Developmental Studies Hybridoma Bank (DSHB), DSHB Cat# E7, RRID:AB_528499, Lot#2/13/20-54 $\mu\text{g}/\text{mL}$ (Schneider, 2012) to detect tubulin in cilia, 1E11 (DSHB Cat# 1E11, RRID:AB_2617214, Lot #3/26/14-30 $\mu\text{g}/\text{mL}$) and SynB (from Dr. Gary Wessel, Brown University) to detect sea urchin SynB-expressing neurons (Burke et al., 2006; Leguia, Conner, Berg, & Wessel, 2006; Junko Yaguchi, Angerer, Inaba, & Yaguchi, 2012; S. Yaguchi et al., 2011), serotonin (Sigma-Aldrich Cat# S5545, RRID:AB_477522) (Buznikov, Peterson, Nikitina, Bezuglov, & Lauder, 2005; Squires et al., 2010). Embryos were fixed in 4% paraformaldehyde (PFA) (20% stock; EMS, Hatfield, PA) in artificial sea water overnight at 4°C. Three 15-min Phosphate Buffered Saline-Tween-20 0.05% (PBST) (10X PBS; Bio-Rad, Hercules, CA) washes were performed. Embryos were blocked with 4% sheep serum (MilliporeSigma, St. Louis, MO) for 1 h at RT. For 1E11, the embryos were fixed in 4% PFA for 10 min and post fixed with 100% acetone for 1 min and washed with PBST containing 0.1% Triton X-100 (Thermo Fisher Scientific, Waltham, MA), and incubated with the antibody for two nights at 4°C in blocking buffer (10% Bovine serum albumin (MilliporeSigma, St. Louis, MO) in PBST-0.1% Triton X-100). For SynB antibody, we fixed embryos with 3.7% formaldehyde in filtered neutral sea water (FSW) for 20 min at RT and 1 min post fix with ice-cold methanol and washed with PBST-0.1% Triton X-100 and incubated overnight. Primary antibody incubation was performed with Endo1, 1E11, SynB, serotonin, at 1:50, 1:2, 1:200, and 1:500, respectively. Corresponding negative controls were set up the same way without the primary antibody. Embryos were washed three times for 15 min with PBST followed by incubation with secondary antibodies goat anti-mouse (for Endo1 and 1E11) and goat anti-rabbit (for SynB and Serotonin) Alexa 488 or Alexa 647 at 1:300 for 1 h at

RT (Thermo Fisher Scientific, Waltham, MA). For tubulin immunolabeling, control embryos were injected with a non-fixable FITC and the miR-124 inhibitor-injected embryos were injected with fixable Texas Red. Control and miR-124 inhibitor-injected embryos were immunolabeled with tubulin in both separate and the same wells to make sure the differences observed were not due to potential technical differences.

The Phalloidin conjugated to Alexa 488 (Thermo Fisher Scientific, Waltham, MA) was resuspended in 100% methanol to make 200 U/ml stocks and then lyophilized and resuspended in PBST-0.1% Triton-X-100 to make a final concentration of 10 U/ml, which was added to the embryos. Embryos were fixed in 4% PFA in 1XPBS for 5 min on ice and then placed at RT for 15 min. They were post-fixed in 100% acetone for 10 min on ice and washed with PBST-0.1% Triton-X-100, followed by incubation with Phalloidin for 1 h at RT and three washes with PBST and then 1XPBS. All immunolabeled embryos were imaged using a Zeiss LSM 880 scanning confocal microscope (Carl Zeiss Incorporation, White Plains, NY) (Zeiss LSM 880 with Airyscan Confocal Laser Scanning Microscope (RRID:SCR_020925)). All immunolabeled embryos were mounted using DAPI in PBST buffer (NucBlue; Thermo Fisher Scientific, Waltham, MA). The maximum intensity projections of Z-stack images were acquired with Zen software (Carl Zeiss Incorporation, White Plains, NY) and processed with Adobe Photoshop (RRID:SCR_014199) and Adobe Illustrator (Adobe, San Jose, CA) (RRID:SCR_010279).

Quantification

To measure the levels of miR-124, 1E11, serotonin, and tubulin (protein and RNA) in each embryo, we took maximum intensity projections and exported them into ImageJ (Schneider, 2012) (National Center for Microscopy and Imaging Research: ImageJ Mosaic Plug-ins, RRID:SCR_001935). The serotonin and 1E11 containing region in the ciliary band was measured with the background subtracted. For tubulin, we measured the whole embryo and subtracted the background from it. For miR-124 levels, that average fluorescent intensity was calculated by measuring the area of the embryo of interest and subtracting the average fluorescent background. All the embryos were measured in the same orientation for consistency. All presented fluorescent images are maximum intensity projections. Colorimetric

and DIC images are single slices. Unless stated otherwise, SEM is graphed, and Student t-test was used for all experiments.

To measure gut contraction, we mounted the embryos on protamine sulfate coverslips in FSW. The sides of the coverslip were sealed with melted petroleum jelly. Each embryo was recorded for four mins using Observer Z.1 microscope (Carl Zeiss Incorporation, White Plains, NY) (Zeiss Axio Observer (RRID:SCR_021351)) 40X lens, and the number of contractions were counted. The gut contraction was determined by the foregut opening into the midgut as a full contraction. Each video is composed of four frames per sec. Still frame images of embryos during gut contractions are depicted in the figures.

To track swimming movement, we used the manual tracking plugin in ImageJ to obtain velocity (Schneider, 2012) (National Center for Microscopy and Imaging Research: ImageJ Mosaic Plug-ins, RRID:SCR_001935). We set the time interval at 60 sec and the x/y calibration at 0.645 μm . Each movie was imaged for 60 secs and only embryos that stayed in the field of view were analyzed. We tracked the leading edge of the larvae (the top of the mouth) and followed it through the entire movie. To compose the movies, we used four frames per second, consisting of a total of 60 frames for a 15-sec video. Still frame images of embryos during gut contractions are depicted in the figures.

To assess the beating of the cilia, polybead dyed blue 1 μm microspheres were used (Polyscience Inc, Warrington, PA). Embryos were injected with either FITC or Texas Red dextrans and mounted on the same coverslip to limit the variability of beads between control and perturbed embryos. The polybeads were used at 1:500 in sea water. Prior to its use, the beads were sonicated in a water bath for 20 min. We mounted the control and experimentally treated embryos with the diluted polybeads and image them using Observer Z.1 microscope (Carl Zeiss Incorporation, White Plains, NY) (Zeiss Axio Observer (RRID:SCR_021351)) for two mins. To quantify the ciliary beating flow videos, we drew a rectangle 15 μm x 60 μm positioned 15 μm away from the mouth of the embryo. The beads were counted as they entered the imaging area, and the number of beads was normalized to the control. To subtract background flow, embryos were deciliated with 2X sea water for five min, then washed with normal sea water, then imaged with diluted polybeads as described above. Before normalization, the average number of beads entering the

region of interest of the deciliated larvae was subtracted from the average number of beads entering the region of interest of the control and experimentally treated embryos.

Cloning of constructs for luciferase assays

The CDS of *NeuroD1* and 3'UTR of *Notch* were cloned using sea urchin cDNA into Zeroblunt vector (Table 1) (Thermo Fisher Scientific, Waltham, MA). Plasmids containing potential cloned DNA inserts were subjected to DNA sequencing (Genewiz Services, South Plainfield, NJ). *NeuroD1* CDS and *Notch* 3'UTR were subcloned downstream of the *Renilla* luciferase (*RLUC*) as described previously (N. Stepicheva et al., 2015). miR-124 seed sequence was deleted from the *NeuroD1* CDS, by using the QuikChange Lightning Kit (Agilent Technologies, San Jose, CA). The miR-124 binding sites within the 3'UTR of *Notch* were mutagenized at the third and fifth binding sites (Staton & Giraldez, 2011). The sequence of the mutagenesis primers used is listed in Table 1. Clones were sequenced to check for the deleted or mutated miR-124 binding site (Genewiz Services, South Plainfield, NJ). *NeuroD1 RLUC* reporter constructs primers, restriction enzymes, and RNA polymerases used are listed in Table 1. Firefly construct (*FF*) was linearized using *SpeI* and *in vitro* transcribed with SP6 RNA polymerase (N. Stepicheva et al., 2015). Transcripts were purified using the RNA Nucleospin Clean-up kit (Macherey-Nagel, Bethlehem, PA). *FF* and reporter *RLUC* constructs were co-injected at 50 ng/ μ L. 25 embryos at the mesenchyme blastula stage (24 hpf) were collected in 25 μ L of 1X Promega passive lysis buffer and vortexed at RT. Dual-luciferase assays were performed using the Promega™ Dual-Luciferase™ Reporter (DLR™) Assay Systems with the Promega™ GloMax™ 20/20 Luminometry System (Promega, Madison, WI). The rest of the assay was performed as previously described (N. Stepicheva et al., 2015).

Preparation of RNA transcripts for injections

NeuroD1 CDS was *in vitro* transcribed with Sp6 mMessage (Thermo Fisher Scientific, Waltham, MA). Transcripts were purified using the RNA Nucleospin Clean-up kit (Macherey-Nagel, Bethlehem, PA). The *in vitro* transcribed *NeuroD1* was injected at 1, 2, and 3 μ g/ μ L with cytoplasmic *mCherry* RNA as control (Gustafson, Yajima, Juliano, & Wessel, 2011) at 3, 2, and 1 μ g/ μ L, respectively. The RNA was passed through a spin column (MilliporeSigma, St. Louis, MO) prior to injection. The

control injection solution contained 4 $\mu\text{g}/\mu\text{L}$ of *mCherry*, which allowed us to detect potential RNA degradation *NeuroD1* transcript. The *mCherry* control and *NeuroD1* transcript were injected at 2 $\mu\text{g}/\mu\text{L}$ for subsequent experiments, based on the dose-response experiment.

TUNEL assay

The steps performed for TUNEL assay are as described previously with modifications (Vega Thurber & Epel, 2007). We treated physiological embryos at different developmental time points when the neuronal progenitor cells undergo their last mitotic division (46 hpf, 48 hpf, 50 hpf, 52 hpf), according to previous literature (Garner et al., 2016; Mellott et al., 2017). We determined that 50 hpf and 52 hpf resulted in increased apoptosis compared to the other time points (data not shown). The negative control did not contain any of the TUNEL enzyme. For the positive control for apoptosis, embryos were treated with DNase (Vega Thurber & Epel, 2007). Injected embryos were fixed in 4% PFA, 100mM HEPES in FSW for 15 min at room temperature and then a 10 min post-fix at room temperature with 2:1 ethanol: glacial acidic acid. Embryos were then washed with 1XPBS three times at room temperature and incubated for 1 h with TUNEL labeling mix at 37°C in a humid chamber. TUNEL labeling mix was made as described by the manufacturer (MilliporeSigma, St. Louis, MO). The embryos were washed 3 times with 1XPBS at room temperature and DAPI was added before they were mounted and imaged (NucBlue; Thermo Fisher Scientific, Waltham, MA). The embryos were imaged using a Zeiss LSM 880 scanning confocal microscope (Carl Zeiss Incorporation, White Plains, NY) (RRID:SCR_020925). The maximum intensity projections of Z-stack images were acquired with Zen software (Carl Zeiss Incorporation, White Plains, NY) (RRID:SCR_020925) and processed with Adobe Photoshop (RRID:SCR_014199) and Adobe Illustrator (Adobe, San Jose, CA) (RRID:SCR_010279).

Results

NeuroD1 influences *SoxC*, *Delta*, *Brn1/2/4*, and *Elav* transcript levels.

NeuroD1 has been shown to play an evolutionarily conserved role in neurogenesis by promoting neuronal differentiation, as well as in reprogramming differentiated non-neuronal cells into neurons (Morrow, Furukawa, Lee, & Cepko, 1999; Tutukova et al., 2021). We bioinformatically identified *NeuroD1* transcript to

contain one miR-124 binding site. Prior to examining miR-124's post-transcriptional regulation of neurogenesis, we first examined the function of *NeuroD1*. We determined that the expression of *NeuroD1* is low in early developing embryos and peaks at gastrulation, followed by decreased expression during the larval stage (Fig. 1B).

To test the function of *NeuroD1*, we performed loss-of-function studies of *NeuroD1* with a translation-blocking morpholino (*NeuroD1* MASO). To determine the role of *NeuroD1* during neurogenesis, we assayed transcript levels of genes that encode key TFs and signaling components of the neuronal GRN in *NeuroD1* MASO and control MASO-injected embryos in gastrula and larval stages, at the time when *NeuroD1* is expressed. We observed that during the gastrula stage, the expression of *Delta* was increased 2-fold (Fig. 1C). During the larval stage, the expression levels of *SoxC*, *Delta*, *Brn1/2/4*, and *Elav* were decreased at least 2-fold (Fig. 1C). To further understand *NeuroD1*'s regulation of *Delta*, we examined the spatial expression of *Delta* in control and *NeuroD1* MASO-injected embryos. We observed that *NeuroD1* MASO-injected gastrulae have more *Delta*-expressing cells, whereas *NeuroD1* MASO-injected larvae have less *Delta*-expressing cells (Fig.S1). Thus, the *Delta* FISH data recapitulated the qPCR data, with the assumption that each cell expresses similar number of *Delta* transcripts (Figs. 1C and S1).

We also examined the mature neuronal network with the sea urchin SynB antibody, which recognizes mature, functional neurons (Burke et al., 2006; Leguia et al., 2006). *NeuroD1* inhibition resulted in a significant decrease in SynB-expressing neurons along the ciliary band and the mouth (Fig. 1D).

miR-124 is enriched in the ciliary band where neurons reside.

With *NeuroD1* integrated into the neuronal GRN, we then investigated the expression pattern of miR-124 throughout development. Results indicate that miR-124 is not detectable until the morula stage (Fig. 2A). In the blastula and gastrula stages, miR-124 is expressed ubiquitously. Later in the larval stage, miR-124 is enriched within ciliary band on the lip region (Fig. 2A). Specifically, miR-124 is expressed in basal epithelial cells, similar to where SynB-positive neurons are localized, juxtaposed to cells that express *Onecut* (Fig. 2B) (Burke, Moller, Krupke, & Taylor, 2014).

Inhibition of miR-124 leads to endodermal and mesodermal developmental defects.

To test the loss-of-function of miR-124, we microinjected miR-124 inhibitor into zygotes. Embryos injected with the miR-124 inhibitor have a significant reduction of miR-124 levels, compared to injected control embryos, indicating the effectiveness of the inhibitor (Fig. 3A). We observed a dose-dependent severity of miR-124 inhibitor-induced phenotypes, ranging from a developmental delay, endodermally-derived gut morphological defects, or delayed formation of mesodermally-derived coelomic pouches (with *Vasa*-expressing cells in the archenteron, Fig. S2A), clusters of cells in the blastocoel of gastrulae, and combinations of these defects (Fig. 3B). Of note is that coelomic pouches with *Vasa*-expressing cells are present at the larval stage (72 hpf), indicating that miR-124 depletion induced a transient delay in their formation (Fig. S2B).

Inhibition of miR-124 results in defects in gut contractions and cardiac sphincter.

One of the morphological changes we observed in miR-124 inhibitor-injected gastrulae is that they had a wider gut compared to the control (Fig. 3B). miR-124 inhibitor-injected gastrulae had delayed expression of *Endo1*, which is expressed specifically in the midgut and hindgut, and recovered by the larval stage (Fig. 4A-B) (Wessel & McClay, 1985). These gastrula gut defects were rescued with a co-injection of the miR-124 inhibitor and a miR-124 mimic, indicating that these defects are specifically induced by the miR-124 inhibitor at the gastrula stage. In addition, we found that miR-124 inhibition results in decreased gut contractions compared to the control larvae (Fig. 4C, Video 1-3).

To elucidate potential mechanisms of the gut defects, we examined the expression of *FoxA* and *Krl*, which are TFs important for endodermal specification (Oliveri, Walton, Davidson, & McClay, 2006; Yamazaki et al., 2008). Results indicate that the expression of *FoxA* and *Krl* does not change significantly (Fig. S3). In addition, we found that differences in gut contractions are not likely due to filamentous actin structures of the circumpharyngeal muscles as overall the filaments appeared to be organized (Fig. 4D). However, miR-124 inhibitor-injected larvae have a significantly wider cardiac sphincter compared to the control (Fig. 4D). Thus, defects in gut contractions of miR-124 inhibitor-injected larvae may be partially due

to the cardiac sphincter defects and/or neuronal network of the gut. The mechanism of miR-124 inhibitor-induced gut defects still needs to be elucidated.

miR-124 regulates larval swimming.

Sea urchin larval swimming is driven by the beating of the cilia in cells of the ciliary band and is regulated by several neurotransmitters, including serotonin, dopamine, and γ -aminobutyric acid (Devlin, 2001; Squires et al., 2010; Yoshihiro, Keiko, Chieko, Akemi, & Baba, 1992). We observed a significant decrease in the swimming velocity (distance/time) in the miR-124 inhibitor-injected larvae compared to the control (Fig. 5A, Video 3-5). The swimming defect in miR-124 inhibitor-injected larvae was rescued with a miR-124 mimic co-injection, indicating that this swimming defect is specifically induced by miR-124 inhibition (Fig. 5A, Video 3-5). Of note is that although the larvae have not fully developed their pre- and post-oral arms in both control and miR-124 inhibitor-injected larvae, the control larvae still swam with significantly higher velocity than the miR-124 perturbed larvae.

We further assessed the effectiveness of ciliary beating by counting the number of polybeads propelled by the larval cilia in the anterior region of the control or miR-124 inhibitor-injected larvae. Results indicate that miR-124 inhibitor-injected larvae are less effective at ciliary beating (Fig. 5B, Video 6-8). Using tubulin immunolabeling, we did not observe differences in the morphology of the cilia between the miR-124 inhibitor-injected and the control larvae. However, a significant increase in tubulin levels was consistently observed in the miR-124 inhibitor-injected larvae compared to the control (Fig. 5C). We also observed that the expression of *Onecut* was dramatically decreased in miR-124 inhibitor-injected larvae (Fig. 5D).

Inhibition of miR-124 leads to decreased mature neurons.

Serotonin has been found to mediate sea urchin gut contractions and larval swimming (Wada, Mogami, & Baba, 1997; Junko Yaguchi & Yaguchi, 2021). Since we observed gut contraction and swimming defects, we examined serotonin. Results indicate that while the number of serotonergic neurons stayed the same in miR-124 inhibitor-injected larvae compared to the control, the overall level of serotonin in the miR-124 inhibitor-injected larvae was significantly decreased and serotonergic neurons had fewer dendritic spines (Fig. 6A). Additionally, miR-124 inhibition resulted in a significant decrease in SynB-expressing neurons along the ciliary band and the mouth (Fig. 6B). This decrease in mature neurons was rescued with a co-

injection of miR-124 inhibitor with a miR-124 mimic, indicating that the observed neuronal defects are specifically induced by the miR-124 inhibitor.

miR-124 modulates neuronal GRN to regulate specification, differentiation, and maturation of neurons.

To systematically examine the function of miR-124 on the specification, differentiation, and maturation of neurons, we tested the spatial, temporal, and/or levels of expression of neuronal GRN components in control and miR-124 inhibitor-injected embryos. *Wnt6* and *FGFA* transcripts were 2-fold decreased in miR-124 inhibitor-injected embryos compared to the control (Fig. 6C). SoxB1 is a TF at the top of the neuronal GRN hierarchy, regulating all three domains of the nervous system (Lynne M. Angerer, Newman, & Angerer, 2005). miR-124 inhibitor-injected blastulae had no change in *SoxB1* expression compared to the control (Figs. 6C, 6D). Downstream of SoxB1 is *Foxq2*, which is important for early establishment of the neuronal apical domain and serotonergic neuron development (Lynne M. Angerer et al., 2005). A significant expansion of *Foxq2* expression was observed in the miR-124 inhibitor-injected embryos compared to the control (Fig. 6E), while the level of *Foxq2* transcripts did not significantly change (Fig. 6C). The expansion of *Foxq2* expression is a result of increased number of *Foxq2*-expressing cells in the miR-124 inhibitor-injected embryos. On average, the *Foxq2*-expressing cells in the miR-124 inhibitor-injected embryos have less intensity of fluorescence compared to the *Foxq2*-expressing cells of the control (Fig. 6E). This result suggests that while the number of *Foxq2*-expressing cells are increased in miR-124 inhibitor-injected embryos, each of the cell potentially expresses less *Foxq2* transcript, since the overall level of *Foxq2* is decreased in miR-124 inhibitor-injected embryos compared to the control (Fig. 6E, 6C). Downstream of *Foxq2* is SoxC, which is important for the development of neurons in the apical domain and expressed in the endomesoderm (Burke et al., 2014; L. A. Slota, Miranda, & McClay, 2019). The miR-124 inhibitor-injected larvae had a significant increase in SoxC expression in the endomesoderm region compared to the control at the blastula stage but did not change in the apical domain, suggesting that miR-124 may have an additional function in the endomesoderm (Fig. 6F) (Perillo et al., 2018; Z. Wei et al., 2011). Overall, the level of SoxC in the blastula was not significantly altered by miR-124 perturbation (Fig. 6F). Later, the SoxC-positive neuronal progenitor cells also express *Brn1/2/4*

(Garner et al., 2016). miR-124 inhibitor-injected gastrulae have an increased number of *SoxC* and *Brn1/2/4*-expressing cells (Fig. 6G). Once the neuronal *SoxC*-positive progenitors undergo their last mitotic division, the two daughter cells contain varying levels of Delta and Notch proteins (Garner et al., 2016; Mellott et al., 2017). The differentiated neurons become *Delta* and *Brn1/2/4*-positive while the other daughter cell containing more Notch will become apoptotic (Burke et al., 2014). We did not observe any change in the number of *Delta*-expressing cells at the gastrula stage (Fig. 6G). However, miR-124 inhibition resulted in an increase of *SoxC* and *Brn1/2/4*-positive cells in the gastrulae that persisted to the larvae, indicating that miR-124 has a broad impact on several TFs regulating the neuronal differentiation process (Figs. 6C-H). We further tested the number of *Elav*-expressing cells to examine neuronal maturation (Garner et al., 2016). We observed that the number of *Elav*-expressing cells is significantly fewer in the miR-124 inhibitor-injected larvae compared to the control (Fig. 6H). Overall, these results indicate that miR-124 inhibition led to an increased number of cells expressing neuronal specification and differentiation factors and a concomitant decrease of mature and functional neurons.

miR-124 directly suppresses components of neuronal GRN.

To determine the molecular mechanism of miR-124's regulation of neurogenesis and larval behavior, we bioinformatically identified two miR-124 binding sites (or seed sequences) within the 3' UTR of *Notch* and one miR-124 binding site within the coding sequence of *NeuroD1*. We cloned *Notch* and *NeuroD1* downstream of *Renilla Luciferase (RLUC)* reporter construct. Site-directed mutagenesis was used to disrupt miR-124 binding at predicted sites within *Notch* and *NeuroD1*. The dual-luciferase assay results indicate that miR-124 directly suppresses the first binding site of *Notch* and *NeuroD1* (Fig. 7A). To determine the impact of removing miR-124's suppression of *NeuroD1* and/or *Notch*, we injected a morpholino-based target protector (TP) (Rensburg et al., 2019; Staton & Giraldez, 2011) that is complementary to the validated miR-124 binding site and flanking sequences within *NeuroD1* and/or *Notch*. We also designed control TPs that do not bind to the miR-124 binding site but in another region of either *Notch* or *NeuroD1* transcript. Of note is that all the designed TPs were blasted against the sea urchin genome and are homologous only to the sites we designed against. To determine the specificity of our *Notch* TP and *NeuroD1* TP, we injected either *Notch* or

NeuroD1 wildtype *RLUC* reporter construct with or without the *Notch* or *NeuroD1* TPs (against miR-124 binding site), as well as the negative control against human β -globin, control *Notch* TPs or control *NeuroD1* TPs. We determined that embryos injected with *Notch* or *NeuroD1* TPs against the miR-124 sites, have a significantly higher luciferase readout compared to all control TPs. Embryos injected with *Notch* or *NeuroD1* wildtype *RLUC* reporter constructs with the *Control Notch* or *NeuroD1* TPs that bind *Notch* or *NeuroD1* transcripts (but not miR-124 binding site) have a similar basal luciferase signal as the negative control β -globin control TP-injected embryos. (Fig. S4A). These results indicate that our *Notch* and *NeuroD1* TPs are specifically blocking the validated miR-124 binding sites.

Removing miR-124's direct suppression of *NeuroD1* results in gut contraction and swimming defects.

Since the regulatory role of the Delta/Notch signaling pathway and miR-124's regulation of *Notch* on neuronal development have been examined previously (Chen et al., 2011; Mellott et al., 2017), we focus here on examining miR-124's regulation of *NeuroD1*. This *NeuroD1* TP prevents the endogenous miR-124 from binding to the *NeuroD1* to mediate post-transcriptional repression. Removing miR-124 suppression of *NeuroD1* resulted in a trend of decreased gut contractions (Fig. 7B, Video 9-10). Zygotes injected with exogenous *NeuroD1* transcripts to mimic the effect of blocking miR-124's suppression of *NeuroD1* resulted in a significant decrease in gut contractions, indicating that *NeuroD1* overexpression (OE) is sufficient to result in aberrant gut contractions (Fig. S5, Video 11-12).

Results indicate that *NeuroD1* TP-injected larvae displayed similar swimming defects as miR-124 inhibitor-injected larvae and *NeuroD1* OE larvae (Figs. 5A, Video 3-5; 7C, Video 13-14; S5B, Video 15-16). *NeuroD1* TP-injected larvae also exhibit decreased efficacy in cilia beating, as assayed by the larvae's ability to propel beads (Fig. 7D, Video 17-18). Removal of miR-124's suppression of *NeuroD1* results in a slight increase in tubulin, similar to what we observed in miR-124 inhibitor-injected larvae (Fig. 7E).

Blocking miR-124's suppression of *NeuroD1* results in fewer functional neurons and more *Elav*-expressing cells.

Similar to miR-124 inhibitor-injected larvae, *NeuroD1* TP-injected embryos have a significant decrease in the overall level of serotonin, while the number of

serotonin-expressing cells stays the same (Fig. 8A). A decrease in serotonin levels was also observed in *NeuroD1* OE larvae (Fig. S6C). In addition, blocking miR-124's suppression of *NeuroD1* results in a significant decrease in SynB-expressing neurons along the ciliary band and the mouth (Fig. 8B). This change in SynB-positive neurons was also observed in the *NeuroD1* OE larvae (Fig. S5D).

To further reveal the impact of miR-124's suppression of *NeuroD1*, we systematically examined the spatial expression of factors of the neuronal GRN. All of the major neuronal factors in *NeuroD1* TP-injected blastulae have increased trend of expression, with *Wnt6* greater than 2-fold increase, compared to the control (Fig. 8C). The spatial expression of *Foxq2* is similar between *NeuroD1* TP or control TP-injected blastulae (Fig. 8D).

NeuroD1 TP-injected gastrulae exhibit no change in the number of *SoxC* and *Delta*-expressing cells and consistently have one additional *Brn1/2/4*-expressing cell compared to the control (Fig. 8E). However, *NeuroD1* TP-injected larvae have a significant increase in the numbers of *SoxC*, *Brn1/2/4*, and *Elav*-expressing cells compared to the control (Fig. 8F).

miR-124 regulates *Notch* and *NeuroD1* in the neuronal GRN

To determine the specificity of the miR-124 inhibitor on *Notch* and *NeuroD1*, we injected either *Notch* or *NeuroD1* wildtype *RLUC* reporter constructs with or without the miR-124 inhibitor (Fig. S4B). We observed that miR-124 inhibitor-injected embryos had a significant increase in translated RLUC compared to the control, indicating that the miR-124 inhibitor is effective in specifically suppressing *Notch* and *NeuroD1* RLUC translation (Fig. S4B). The increased number of *Elav*-expressing cells in *NeuroD1* TP-injected larvae contrasts with the decreased number of *Elav*-expressing cells in miR-124 inhibitor-injected embryos (Figs. 6G, 8F). To resolve this difference, we co-injected *NeuroD1* TP with *Notch* TP to test the effects of removing miR-124's suppression of both transcripts and assayed for changes in the number of *Elav*-expressing cells. Results indicate that co-injection of *NeuroD1* TP and *Notch* TP recapitulate the decrease in *Elav*-expressing cells observed in miR-124 inhibitor-injected embryos (Figs. 6G, 9A). To test the hypothesis that removal of miR-124 suppression of *Notch* results in fewer *Elav*-positive cells as a result of increased Notch that induces apoptosis of neural progenitor cells, we examined the number of apoptotic cells in *control* TP or *Notch* TP-injected larvae at 52 hpf when the neural

progenitor cells undergo their last mitotic asymmetric division (Garner et al., 2016; Mellott et al., 2017). We observed that *Notch* TP-injected embryos have a significant number of apoptotic cells compared to the *control* TP embryos (Fig. 9B).

Discussion

We integrated *NeuroD1* into the neuronal GRN and identified that its perturbation correlates with transcript level changes of *SoxC*, *Delta*, *Brn1/2/4*, and *Elav* (Figs. 1C, 10). With a more complete neuronal GRN, we systematically examined the post-transcriptional regulation mediated by miR-124. We discovered that miR-124 regulates gut contractions, swimming behavior, and neuronal development. The molecular mechanism of miR-124's regulation of neurogenesis is in part through its suppression of *Notch*, which mediates differentiation of progenitor neurons (Garner et al., 2016; Mellott et al., 2017). miR-124 also suppresses *NeuroD1*, which we find to be important in mediating the transition between differentiation and maturation of neurons. Overall, this study contributes to our understanding of miR-124's prolific regulatory role in neuronal specification, differentiation, and maturation.

Previously, it has been observed that *NeuroD1* is expressed in the larval ciliary band and gut (Perillo et al., 2018). In vertebrates, in addition to its function in neurogenesis, *NeuroD1*'s loss-of-function results in severe diabetes, revealing *NeuroD1*'s additional function in the pancreas (Kamath, Chen, Enkemann, & Sanchez-Ramos, 2005). Interestingly, cells with a pancreatic-like signature are localized within the sea urchin embryonic gut and express similar TFs as neurons during development (Perillo et al., 2018; Perillo, Wang, Leach, & Arnone, 2016). Additional TFs that belong to this category include *SoxC* and *Brn1/2/4*, which are expressed in the apical domain, ciliary band, and the larval gut (Garner et al., 2016; Perillo et al., 2018; S. Yaguchi et al., 2011). It was proposed that these pancreatic endocrine cells in the larval gut may have co-opted some neuronal regulatory factors from an ancestral neuron (Perillo et al., 2018). Although we do not understand the regulatory mechanism of *NeuroD1* on *Delta* expression, the number of *Delta*-expressing cells correlated with the level of qPCR, if the number of *Delta* transcripts expressed by each cell is similar (Fig. 1C, S1). Recently, it has been shown that an overexpression of *NeuroD1* in zebrafish embryos leads to increased expression of *Delta* ligands (*deltaB*, *deltaC*, and *delta-like4*) during the hatching stage prior to the

larval stage (Kimmel, Ballard, Kimmel, Ullmann, & Schilling, 1995; Reuter et al., 2022). We do not know if zebrafish *NeuroD1* temporally regulates *Delta* differently during various developmental timepoints. Thus, our observation that *NeuroD1* dynamically influence the number of *Delta*-expressing cells at gastrula and larval stages is novel, although the exact mechanism of how this occurs remains unclear.

NeuroD1 MASO-injected larvae resulted in at least a 2-fold increase of *SoxC*, *Delta*, *Brn1/2/4*, and *Elav*, transcripts (Fig. 1C). Thus, in the sea urchin, *NeuroD1* may regulate neuronal development as well as gut functions, since we observed that larvae injected with exogenous *NeuroD1* exhibited a significant decrease in gut contractions (Fig. S6A, Video 11-12). While we observed *NeuroD1* expression peaks during the gastrula stage, we do not know exactly where to place *NeuroD1* within the neuronal GRN, since *SoxC* and *Delta* have earlier expression in the endomesoderm. We can only conclude that *NeuroD1* influences transcript levels of these factors of the neuronal GRN.

To examine the function of miR-124, we injected miR-124 inhibitor into zygotes. One of the defects we observed was decreased gut contractions in miR-124 inhibitor-injected larvae (Fig. 4C, Video 1-2). Since we observe a trend in decreased gut contractions in the *NeuroD1* TP-injected larvae, whereas miR-124 inhibition and *NeuroD1* OE resulted in a significant decrease in gut contractions, this suggests that miR-124 likely regulates *NeuroD1* and an additional unknown factor to impact gut contractions (Figs. 4C, Video 1-2; 7B, Video 9-10; and S5A, Video 11-12). The exact molecular mechanism of how miR-124 regulates gut development and gut contractions is still unknown; however, a potential explanation may be due to decreased level of serotonin (Fig. 6A).

The overall level of serotonin was significantly decreased in the miR-124 inhibitor-injected embryos compared to the control, although we observed no change in their number of serotonergic neurons, suggesting that their specification is not affected by miR-124 perturbation (Fig. 6A). Decreased serotonin levels in miR-124 inhibitor-injected larvae may be due to an expansion of the *Foxq2* expression domain (Fig. 6E). In a different species of sea urchin, increased *Foxq2* expression domain leads to a decreased level of serotonin (J. Yaguchi et al., 2016). *Foxq2* is expressed in the early blastulae and its expression must be suppressed later in gastrulae to allow proper development of serotonergic neurons in the ciliary band (J.

Yaguchi et al., 2016; S. Yaguchi et al., 2008). Thus, ectopic expansion of *Foxq2* in miR-124 perturbed embryos may result in decreased serotonin (Figs. 5A, 6A, 6E). Since serotonin is important for early swimming, feeding behavior, and gut contraction in the larvae, miR-124 inhibition may induce a decrease in serotonin that contributes to the decreased gut contractions and swimming defects (Junko Yaguchi & Yaguchi, 2021; S. Yaguchi & Katow, 2003).

In addition, regulation of larval swimming is in part due to miR-124's direct suppression of *NeuroD1*, since embryos injected with miR-124 inhibitor, *NeuroD1* TP, or *NeuroD1* transcripts, all lead to decreased swimming velocity (Figs. 5A, 7C, S5B). The 3-day old larvae in our culturing conditions do not seem to have fully developed the pre-oral and post-oral arms. The swimming defect is not likely attributed to structural defects of the cilia, as tubulin appears to be normal but interestingly, the level of tubulin significantly increased in miR-124 inhibitor and *NeuroD1* TP-injected larvae (Figs. 5C, 7E). This may be due to miR-124's direct suppression of *NeuroD1*, since it has been observed previously that an increase in *NeuroD1* resulted in increased neuronal-specific tubulin protein, Tuji1 (Boutin et al., 2010). However, the exact mechanism of how increased *NeuroD1* leads to increased tubulin is not known. Together, these results indicate that miR-124's direct suppression of *NeuroD1* impacts larval swimming.

miR-124 plays an evolutionarily conserved function in regulating the balance between neuronal proliferation and differentiation (Ambasudhan et al., 2011; Chen et al., 2011; Kozuka et al., 2019; Makeyev et al., 2007). We found that miR-124 inhibitor-injected larvae had a significant decrease in SynB-expressing neurons (Fig. 6B). This could be a result of decreased *Onecut* expression (Fig. 5D). Decreased *Onecut* expression has been shown to result in decreased neuronal bundling and improper interconnecting axonal tracts in sea urchin larvae (J. Yaguchi et al., 2016; S. Yaguchi, Yaguchi, Angerer, Angerer, & Burke, 2010). Thus, decreased *Onecut* expression may potentially negatively affect the formation of SynB-expressing neurons in their connections in the ciliary band (Figs. 5D, 6B) (Krupke & Burke, 2014; Leslie A. Slota, Miranda, Peskin, & McClay, 2019). How miR-124 mediates the expression of *Onecut* is unknown.

To reveal the molecular mechanism of how miR-124 regulates neurogenesis, we systematically assessed the spatial, temporal, and levels of expression of key

factors in the neuronal GRN in miR-124 perturbed embryos. Results indicate that miR-124 inhibition resulted in decreased expression of *Wnt6* and *FGFA*, indicating that miR-124 is likely to regulate neurogenesis at an early stage when *Wnt6* and *FGFA* specify the neuroectoderm domain in the early blastulae (Fig. 6C). Since neither *Wnt6* nor *FGFA* contains a potential canonical miR-124 binding site, miR-124 is likely to regulate a repressor of *Wnt6* and *FGFA*. Consistent with this hypothesis, *Wnt6* is known to restrict *Foxq2*'s expression domain (S. Yaguchi et al., 2006), so a decrease in *Wnt6* in miR-124 inhibitor-injected embryos may lead to an expansion of *Foxq2* expression domain (Figs. 6C, 6E).

Our results indicate that miR-124's regulation of neurogenesis is broad, spanning specification, differentiation, and maturation of neurons. We identified miR-124 to directly suppress *Notch* (Fig. 7A), consistent with prior findings (Chen et al., 2011; Jiao, Liu, Yao, & Teng, 2017). In the sea urchin, the Delta/Notch signaling has been identified to be important for non-skeletogenic mesodermal cell specification prior to gastrulation, as well as regulating neurogenesis in mediating asymmetric division of differentiating neurons in gastrula and larval stages (Materna, Ransick, Li, & Davidson, 2013; Mellott et al., 2017; Range, Glenn, Miranda, & McClay, 2008). Thus, based on prior literature of Delta/Notch expression and function and our *NeuroD1* expression data (Fig. 1B), we hypothesize that Delta/Notch functions upstream of *NeuroD1* (Fig. 10).

Additionally, miR-124 regulates *NeuroD1* during the transition from neuronal differentiation to maturation. For the most part, removal of miR-124's suppression of *NeuroD1* phenocopies miR-124 inhibitor-induced defects (Figs. 4C, 5A-C, 6, 7B-E, 8). However, while miR-124 inhibitor-injected embryos had an expanded expression domain of *Foxq2*, *NeuroD1* TP-injected embryos did not have a change in an expression domain of *Foxq2* (Figs. 6E, 8D). This is consistent with our finding that the expression of *NeuroD1* peaks in gastrulae, downstream of *Foxq2* (Fig. 1B). In addition, miR-124 inhibitor-injected gastrulae had a significant increase in the number of *SoxC* and *Brn1/2/4*-expressing cells, indicating that miR-124 regulates the transition from neuronal specification to differentiation and may regulate potential unknown functions in the endomesoderm (Fig. 6F) (Garner et al., 2016; Perillo et al., 2018; S. Yaguchi et al., 2011). In contrast, *NeuroD1* TP-injected gastrulae did not have a significant change in the number of *SoxC*-expressing cells and a net change

of one additional *Brn1/2/4*-expressing cell (Fig. 8E). This suggests that the increased number of *SoxC* and *Brn1/2/4*-expressing cells in miR-124 inhibitor-injected embryos is likely due to its regulation of an unknown factor and not due to its regulation of *NeuroD1*. Thus, from the miR-124 inhibition, *NeuroD1* knockdown, and *NeuroD1* TP injection results, we propose that *NeuroD1* is likely to regulate neuronal factors mainly at the late gastrula to larval stages during neuronal differentiation and maturation (Fig. 10).

One additional discrepancy between the miR-124 inhibitor and *NeuroD1* TP-injected embryos is that miR-124 inhibitor-injected larvae have decreased *Elav*-expressing and SynB-positive neurons compared to control larvae, while *NeuroD1* TP-injected larvae have increased *Elav*-expressing cells and concomitant decrease of SynB-positive neurons (Figs. 6G, 8F). The increase in *Elav*-expressing cells in the *NeuroD1* TP-injected embryos is consistent with decreased *Elav* expression in *NeuroD1* MASO-injected embryos, indicating that *NeuroD1* positively influences *Elav* (Figs. 1C, 8F). miR-124 has been observed in *Xenopus* embryos to inhibit *NeuroD1* in the forebrain and optic vesicle, which resulted in an increased number of cells undergoing mitosis (Kamath et al., 2005). In addition, *NeuroD1* promotes the formation of neuron-like progenitor cells by converting epithelial cells to a neural fate (Matsuda et al., 2019; Pataskar et al., 2016). Thus, the increased number of *Elav*-expressing cells in *NeuroD1* TP-injected larvae may be due to *NeuroD1*'s function in enhancing proliferation and/or promoting the formation of neuron-like cells that may not be functional (Fig. 8F). This is consistent with our results that despite an increase in *Elav*-expressing cells, *NeuroD1* TP-injected larvae have an overall loss of SynB-positive, mature, and functional neurons (Figs. 8B, 8F).

To further dissect the function of miR-124, we co-injected *Notch* TP and *NeuroD1* TPs into zygotes and observed that these larvae have a similar number of *Elav*-expressing cells as miR-124 inhibitor-injected larvae. These results indicate that miR-124's suppression of *Notch* is in part responsible for the decrease in *Elav*-expressing cells in miR-124 inhibitor-injected embryos (Fig. 9A). We determined that removing miR-124's suppression of *Notch* results in increased apoptotic cells (Fig. 9B). A potential explanation for this observation is that removing miR-124's suppression of *Notch* leads to increased Notch protein. In turn, this increased Notch signaling in neural progenitor cells may lead to increased apoptosis (McClay et al.,

2018; Mellott et al., 2017; Pérez, Venkatanarayan, & Lundell, 2022). As a result, in miR-124 inhibitor-injected embryos, fewer neurons are left for NeuroD1 to convert them to *Elav*-expressing cells, and subsequently, fewer SynB-positive neurons (Fig. 8B). The caveat is that although results indicate that removal of miR-124 suppression of *Notch* results in increased number of apoptotic cells and correlate with fewer mature neurons in miR-124 inhibitor-injected embryos, we do not have direct evidence for increased Notch and we do not have evidence that the apoptotic cells are neural progenitor cells. We cannot immunolabel TUNEL-treated embryos with neural antibodies to demonstrate a direct relationship. Nevertheless, overall, these data indicate that miR-124 regulates both *Notch* and *NeuroD1* to mediate proper neurogenesis.

Overall, we have integrated NeuroD1 into the neuronal network and determined that miR-124 regulates specification, differentiation, maturation, and the formation of functional neurons during development, in part by mediating *Notch* and *NeuroD1* (Fig.10). Based on our results, miR-124 is likely to regulate an unidentified factor that inhibits *Wnt6*, *FGFA*, and subsequently increases *Foxq2* expression during neuronal specification. miR-124 also regulates another unknown factor that activates *SoxC* and *Brn1/2/4* during neuronal differentiation in the gastrula stage. miR-124 represses *Notch*, to regulate the differentiation of neurons. In the late gastrula to larval stages, miR-124 suppresses *NeuroD1* to mediate the transition between differentiation and maturation. miR-124 suppresses *NeuroD1* at the larval stage to prevent excessive neural differentiation, allowing already committed neuronal cells to mature into functional neurons. Using the sea urchin embryo, we are able to systematically integrate miR-124's post-transcriptional regulation of the neuronal GRN and reveal miR-124's mechanism of regulation. Overall, we identify miR-124 to have a prolific regulatory role throughout neurogenesis. Since miR-124, Notch, and NeuroD1 are evolutionarily conserved, these results may be applicable to our understanding of neurogenesis in other animals.

References

Amador-Arjona, A., Cimadamore, F., Huang, C.-T., Wright, R., Lewis, S., Gage, F. H., & Terskikh, A. V. (2015). SOX2 primes the epigenetic landscape in neural precursors enabling proper gene activation during hippocampal neurogenesis.

- Proceedings of the National Academy of Sciences of the United States of America*, 112(15), E1936-E1945. doi:10.1073/pnas.1421480112
- Ambasudhan, R., Talantova, M., Coleman, R., Yuan, X., Zhu, S., Lipton, S. A., & Ding, S. (2011). Direct reprogramming of adult human fibroblasts to functional neurons under defined conditions. *Cell stem cell*, 9(2), 113-118. doi:10.1016/j.stem.2011.07.002
- Angerer, L. M., Newman, L. A., & Angerer, R. C. (2005). SoxB1 downregulation in vegetal lineages of sea urchin embryos is achieved by both transcriptional repression and selective protein turnover. *Development*, 132(5), 999. doi:10.1242/dev.01650
- Angerer, L. M., Yaguchi, S., Angerer, R. C., & Burke, R. D. (2011). The evolution of nervous system patterning: insights from sea urchin development. *Development*, 138(17), 3613-3623. doi:10.1242/dev.058172
- Aquino-Nunez, W., Mielko, Z. E., Dunn, T., Santorella, E. M., Hosea, C., Leitner, L., . . . Hudson, M. L. (2020). cnd-1/NeuroD1 Functions with the Homeobox Gene *ceh-5/Vax2* and Hox Gene *ceh-13/labial* To Specify Aspects of RME and DD Neuron Fate in *Caenorhabditis elegans*. *G3 (Bethesda, Md.)*, 10(9), 3071-3085. doi:10.1534/g3.120.401515
- Arenas-Mena, C., Cameron, A. R., & Davidson, E. H. (2000). Spatial expression of Hox cluster genes in the ontogeny of a sea urchin. *Development*, 127(21), 4631-4643. Retrieved from http://www.ncbi.nlm.nih.gov/entrez/query.fcgi?cmd=Retrieve&db=PubMed&dopt=Citation&list_uids=11023866
- Audouard, E., Schakman, O., René, F., Huettl, R. E., Huber, A. B., Loeffler, J. P., . . . Clotman, F. (2012). The Onecut transcription factor HNF-6 regulates in motor neurons the formation of the neuromuscular junctions. *PLoS One*, 7(12), e50509. doi:10.1371/journal.pone.0050509
- Bartel, D. P. (2009). MicroRNAs: target recognition and regulatory functions. *Cell*, 136(2), 215-233. doi:S0092-8674(09)00008-7 [pii]10.1016/j.cell.2009.01.002
- Bartel, D. P. (2018). Metazoan MicroRNAs. *Cell*, 173(1), 20-51. doi:10.1016/j.cell.2018.03.006
- Boutin, C., Hardt, O., de Chevigny, A., Coré, N., Goebbels, S., Seidenfaden, R., . . . Cremer, H. (2010). NeuroD1 induces terminal neuronal differentiation in olfactory neurogenesis. *Proc Natl Acad Sci U S A*, 107(3), 1201-1206. doi:10.1073/pnas.0909015107
- Braun, M. M., Etheridge, A., Bernard, A., Robertson, C. P., & Roelink, H. (2003). Wnt signaling is required at distinct stages of development for the induction of the posterior forebrain. *Development*, 130(23), 5579-5587. doi:10.1242/dev.00685
- Burke, R. D., Moller, D. J., Krupke, O. A., & Taylor, V. J. (2014). Sea urchin neural development and the metazoan paradigm of neurogenesis. *Genesis*, 52(3), 208-221. Retrieved from <http://www.ncbi.nlm.nih.gov/pubmed/25368883>
- Burke, R. D., Osborne, L., Wang, D., Murabe, N., Yaguchi, S., & Nakajima, Y. (2006). Neuron-specific expression of a synaptotagmin gene in the sea urchin *Strongylocentrotus purpuratus*. *J Comp Neurol*, 496(2), 244-251. doi:10.1002/cne.20939
- Buznikov, G. A., Peterson, R. E., Nikitina, L. A., Bezuglov, V. V., & Lauder, J. M. (2005). The pre-nervous serotonergic system of developing sea urchin

- embryos and larvae: pharmacologic and immunocytochemical evidence. *Neurochem Res*, 30(6-7), 825-837. doi:10.1007/s11064-005-6876-6
- Chen, J. S., Pedro, M. S., & Zeller, R. W. (2011). miR-124 function during *Ciona intestinalis* neuronal development includes extensive interaction with the Notch signaling pathway. *Development*, 138(22), 4943-4953. doi:10.1242/dev.068049
- Cho, J. H., & Tsai, M. J. (2004). The role of BETA2/NeuroD1 in the development of the nervous system. *Mol Neurobiol*, 30(1), 35-47. doi:10.1385/mn:30:1:035
- DeBello, W. M., Betz, H., & Augustine, G. J. (1993). Synaptotagmin and neurotransmitter release. *Cell*, 74(6), 947-950. doi:10.1016/0092-8674(93)90716-4
- Devlin, C. L. (2001). The pharmacology of gamma-aminobutyric acid and acetylcholine receptors at the echinoderm neuromuscular junction. *Journal of Experimental Biology*, 204(5), 887. Retrieved from <http://jeb.biologists.org/content/204/5/887.abstract>
- Garner, S., Zysk, I., Byrne, G., Kramer, M., Moller, D., Taylor, V., & Burke, R. D. (2016). Neurogenesis in sea urchin embryos and the diversity of deuterostome neurogenic mechanisms. *Development*, 143(2), 286-297. doi:10.1242/dev.124503
- Gustafson, E. A., Yajima, M., Juliano, C. E., & Wessel, G. M. (2011). Post-translational regulation by gustavus contributes to selective Vasa protein accumulation in multipotent cells during embryogenesis. *Dev Biol*, 349(2), 440-450. doi:10.1016/j.ydbio.2010.10.031
- Huang, P., Kishida, S., Cao, D., Murakami-Tonami, Y., Mu, P., Nakaguro, M., . . . Kadomatsu, K. (2011). The neuronal differentiation factor NeuroD1 downregulates the neuronal repellent factor Slit2 expression and promotes cell motility and tumor formation of neuroblastoma. *Cancer Res*, 71(8), 2938-2948. doi:10.1158/0008-5472.can-10-3524
- Jiao, S., Liu, Y., Yao, Y., & Teng, J. (2017). miR-124 promotes proliferation and differentiation of neuronal stem cells through inactivating Notch pathway. *Cell & bioscience*, 7, 68-68. doi:10.1186/s13578-017-0194-y
- Kamath, S. G., Chen, N., Enkemann, S. A., & Sanchez-Ramos, J. (2005). Transcriptional profile of NeuroD expression in a human fetal astroglial cell line. *Gene expression*, 12(2), 123-136. doi:10.3727/000000005783992133
- Katow, H., Yaguchi, S., & Kyojuka, K. (2007). Serotonin stimulates [Ca²⁺]_i elevation in ciliary ectodermal cells of echinoplutei through a serotonin receptor cell network in the blastocoel. *Journal of Experimental Biology*, 210(3), 403. doi:10.1242/jeb.02666
- Kengaku, M., & Okamoto, H. (1993). Basic fibroblast growth factor induces differentiation of neural tube and neural crest lineages of cultured ectoderm cells from *Xenopus* gastrula. *Development*, 119(4), 1067-1078. Retrieved from <http://www.ncbi.nlm.nih.gov/pubmed/8306875>
- Kimmel, C. B., Ballard, W. W., Kimmel, S. R., Ullmann, B., & Schilling, T. F. (1995). Stages of embryonic development of the zebrafish. *Developmental dynamics : an official publication of the American Association of Anatomists*, 203(3), 253-310. Retrieved from http://www.ncbi.nlm.nih.gov/entrez/query.fcgi?cmd=Retrieve&db=PubMed&dopt=Citation&list_uids=8589427

- Kozuka, T., Omori, Y., Watanabe, S., Tarusawa, E., Yamamoto, H., Chaya, T., . . . Furukawa, T. (2019). miR-124 dosage regulates prefrontal cortex function by dopaminergic modulation. *Sci Rep*, 9(1), 3445. doi:10.1038/s41598-019-38910-2
- Krupke, O. A., & Burke, R. D. (2014). Eph-Ephrin signaling and focal adhesion kinase regulate actomyosin-dependent apical constriction of ciliary band cells. *Development*, 141(5), 1075-1084. doi:10.1242/dev.100123
- Leguia, M., Conner, S., Berg, L., & Wessel, G. M. (2006). Synaptotagmin I is involved in the regulation of cortical granule exocytosis in the sea urchin. *Molecular reproduction and development*, 73(7), 895-905. doi:10.1002/mrd.20454
- Letunic, I., & Bork, P. (2018). 20 years of the SMART protein domain annotation resource. *Nucleic Acids Res*, 46(D1), D493-d496. doi:10.1093/nar/gkx922
- Letunic, I., Khedkar, S., & Bork, P. (2021). SMART: recent updates, new developments and status in 2020. *Nucleic Acids Res*, 49(D1), D458-d460. doi:10.1093/nar/gkaa937
- Lewis, B. P., Burge, C. B., & Bartel, D. P. (2005). Conserved seed pairing, often flanked by adenosines, indicates that thousands of human genes are microRNA targets. In *Cell* (Vol. 120, pp. 15-20). United States.
- Litsiou, A., Hanson, S., & Streit, A. (2005). A balance of FGF, BMP and WNT signalling positions the future placode territory in the head. *Development*, 132(18), 4051-4062. doi:10.1242/dev.01964
- Liu, K., Liu, Y., Mo, W., Qiu, R., Wang, X., Wu, J. Y., & He, R. (2011). MiR-124 regulates early neurogenesis in the optic vesicle and forebrain, targeting NeuroD1. *Nucleic Acids Res*, 39(7), 2869-2879. doi:10.1093/nar/gkq904
- Makeyev, E. V., Zhang, J., Carrasco, M. A., & Maniatis, T. (2007). The MicroRNA miR-124 promotes neuronal differentiation by triggering brain-specific alternative pre-mRNA splicing. *Mol Cell*, 27(3), 435-448. doi:10.1016/j.molcel.2007.07.015
- Mao, C. A., Agca, C., Mocko-Strand, J. A., Wang, J., Ullrich-Luter, E., Pan, P., . . . Klein, W. H. (2016). Substituting mouse transcription factor Pou4f2 with a sea urchin orthologue restores retinal ganglion cell development. *Proceedings. Biological sciences*, 283(1826), 20152978. doi:10.1098/rspb.2015.2978
- Masoudi, N., Tavazoie, S., Glenwinkel, L., Ryu, L., Kim, K., & Hobert, O. (2018). Unconventional function of an Achaete-Scute homolog as a terminal selector of nociceptive neuron identity. *PLoS Biol*, 16(4), e2004979. doi:10.1371/journal.pbio.2004979
- Materna, S. C., Ransick, A., Li, E., & Davidson, E. H. (2013). Diversification of oral and aboral mesodermal regulatory states in pregastrular sea urchin embryos. *Developmental biology*, 375(1), 92-104. doi:10.1016/j.ydbio.2012.11.033
- Matsuda, T., Irie, T., Katsurabayashi, S., Hayashi, Y., Nagai, T., Hamazaki, N., . . . Nakashima, K. (2019). Pioneer Factor NeuroD1 Rearranges Transcriptional and Epigenetic Profiles to Execute Microglia-Neuron Conversion. *Neuron*, 101(3), 472-485 e477. doi:10.1016/j.neuron.2018.12.010
- McClay, D. R., Miranda, E., & Feinberg, S. L. (2018). Neurogenesis in the sea urchin embryo is initiated uniquely in three domains. *Development*, 145(21), dev167742. doi:10.1242/dev.167742
- Mellott, D. O., Thisdelle, J., & Burke, R. D. (2017). Notch signaling patterns neurogenic ectoderm and regulates the asymmetric division of neural

- progenitors in sea urchin embryos. *Development*, 144(19), 3602.
doi:10.1242/dev.151720
- Minokawa, T., Rast, J. P., Arenas-Mena, C., Franco, C. B., & Davidson, E. H. (2004). Expression patterns of four different regulatory genes that function during sea urchin development. *Gene expression patterns : GEP*, 4(4), 449-456.
Retrieved from http://www.ncbi.nlm.nih.gov/entrez/query.fcgi?cmd=Retrieve&db=PubMed&dot=Citation&list_uids=15183312
- Morrow, E. M., Furukawa, T., Lee, J. E., & Cepko, C. L. (1999). NeuroD regulates multiple functions in the developing neural retina in rodent. *Development*, 126(1), 23. Retrieved from <http://dev.biologists.org/content/126/1/23.abstract>
- Nagahara, H., Vocero-Akbani, A. M., Snyder, E. L., Ho, A., Latham, D. G., Lissy, N. A., . . . Dowdy, S. F. (1998). Transduction of full-length TAT fusion proteins into mammalian cells: TAT-p27Kip1 induces cell migration. *Nat Med*, 4(12), 1449-1452. doi:10.1038/4042
- Oliveri, P., Walton, K. D., Davidson, E. H., & McClay, D. R. (2006). Repression of mesodermal fate by foxa, a key endoderm regulator of the sea urchin embryo. *Development*, 133(21), 4173-4181. doi:133/21/4173 [pii]10.1242/dev.02577
- Otim, O., Amore, G., Minokawa, T., McClay, D. R., & Davidson, E. H. (2004). SpHnf6, a transcription factor that executes multiple functions in sea urchin embryogenesis. *Developmental biology*, 273(2), 226-243.
doi:10.1016/j.ydbio.2004.05.033
- Pataskar, A., Jung, J., Smialowski, P., Noack, F., Calegari, F., Straub, T., & Tiwari, V. K. (2016). NeuroD1 reprograms chromatin and transcription factor landscapes to induce the neuronal program. *Embo j*, 35(1), 24-45.
doi:10.15252/embj.201591206
- Pérez, E., Venkatanarayan, A., & Lundell, M. J. (2022). Hunchback prevents notch-induced apoptosis in the serotonergic lineage of *Drosophila Melanogaster*. *Dev Biol*, 486, 109-120. doi:10.1016/j.ydbio.2022.03.012
- Perillo, M., Paganos, P., Mattiello, T., Cocurullo, M., Oliveri, P., & Arnone, M. I. (2018). New Neuronal Subtypes With a “Pre-Pancreatic” Signature in the Sea Urchin *Strongylocentrotus purpuratus*. *Frontiers in Endocrinology*, 9, 650.
Retrieved from <https://www.frontiersin.org/article/10.3389/fendo.2018.00650>
- Perillo, M., Wang, Y. J., Leach, S. D., & Arnone, M. I. (2016). A pancreatic exocrine-like cell regulatory circuit operating in the upper stomach of the sea urchin *Strongylocentrotus purpuratus* larva. *BMC Evolutionary Biology*, 16(1), 117.
doi:10.1186/s12862-016-0686-0
- Puligilla, C., Dabdoub, A., Brenowitz, S. D., & Kelley, M. W. (2010). Sox2 induces neuronal formation in the developing mammalian cochlea. *J Neurosci*, 30(2), 714-722. doi:10.1523/jneurosci.3852-09.2010
- Rajasethupathy, P., Fiumara, F., Sheridan, R., Betel, D., Puthanveetil, S. V., Russo, J. J., . . . Kandel, E. (2009). Characterization of small RNAs in *Aplysia* reveals a role for miR-124 in constraining synaptic plasticity through CREB. *Neuron*, 63(6), 803-817. doi:10.1016/j.neuron.2009.05.029
- Range, R. C. (2018). Canonical and non-canonical Wnt signaling pathways define the expression domains of Frizzled 5/8 and Frizzled 1/2/7 along the early anterior-posterior axis in sea urchin embryos. *Developmental biology*, 444(2), 83-92. doi:10.1016/j.ydbio.2018.10.003

- Range, R. C., Glenn, T. D., Miranda, E., & McClay, D. R. (2008). LvNumb works synergistically with Notch signaling to specify non-skeletal mesoderm cells in the sea urchin embryo. *Development*, *135*(14), 2445-2454. doi:10.1242/dev.018101
- Remsburg, C., Konrad, K., Sampilo, N.-F., & Song, J. (2019). Analysis of MicroRNA Function. In (Vol. 151): *Methods in Cell Biology*.
- Rentzsch, F., Fritzenwanker, J. H., Scholz, C. B., & Technau, U. (2008). FGF signalling controls formation of the apical sensory organ in the cnidarian *Nematostella vectensis*. *Development*, *135*(10), 1761-1769. doi:10.1242/dev.020784
- Reuter, A. S., Stern, D., Bernard, A., Goossens, C., Lavergne, A., Flasse, L., . . . Voz, M. L. (2022). Identification of an evolutionarily conserved domain in Neurod1 favouring enteroendocrine versus goblet cell fate. *PLoS Genet*, *18*(3), e1010109. doi:10.1371/journal.pgen.1010109
- Rozen, S., & Skaletsky, H. (2000). Primer3 on the WWW for general users and for biologist programmers. *Methods in molecular biology*, *132*, 365-386. Retrieved from http://www.ncbi.nlm.nih.gov/entrez/query.fcgi?cmd=Retrieve&db=PubMed&dopt=Citation&list_uids=10547847
- Schneider, C. A., Rasband, W.S., Eliceiri, K.W. (2012). NIH Image to ImageJ: 25 years of image analysis. In (Vol. 9, pp. 671-675): *Nature Methods*.
- Sethi, A. J., Angerer, R. C., & Angerer, L. M. (2014). Multicolor labeling in developmental gene regulatory network analysis. *Methods Mol Biol*, *1128*, 249-262. doi:10.1007/978-1-62703-974-1_17
- Siebel, C., & Lendahl, U. (2017). Notch Signaling in Development, Tissue Homeostasis, and Disease. *Physiol Rev*, *97*(4), 1235-1294. doi:10.1152/physrev.00005.2017
- Slota, L. A., Miranda, E., Peskin, B., & McClay, D. R. (2019). Developmental origin of peripheral ciliary band neurons in the sea urchin embryo. *Developmental biology*, S0012-1606(0019)30269-30266. doi:10.1016/j.ydbio.2019.12.011
- Slota, L. A., Miranda, E. M., & McClay, D. R. (2019). Spatial and temporal patterns of gene expression during neurogenesis in the sea urchin *Lytechinus variegatus*. *Evodevo*, *10*, 2. doi:10.1186/s13227-019-0115-8
- Song, J. L., Stoeckius, M., Maaskola, J., Friedlander, M. R., Stepicheva, N., Juliano, C., . . . Wessel, G. M. (2012). Select microRNAs are essential for early development in the sea urchin. *Developmental Biology*, *362*(1), 104-113. doi:10.1016/j.ydbio.2011.11.015
- Squires, L. N., Rubakhin, S. S., Wadhams, A. A., Talbot, K. N., Nakano, H., Moroz, L. L., & Sweedler, J. V. (2010). Serotonin and its metabolism in basal deuterostomes: insights from *Strongylocentrotus purpuratus* and *Xenoturbella bocki*. *The Journal of Experimental Biology*, *213*(15), 2647. doi:10.1242/jeb.042374
- Staton, A. A., & Giraldez, A. J. (2011). Use of target protector morpholinos to analyze the physiological roles of specific miRNA-mRNA pairs in vivo. *Nature Protocols*, *6*(12), 2035-2049. doi:10.1038/nprot.2011.423
- Stepicheva, N., Nigam, P. A., Siddam, A. D., Peng, C. F., & Song, J. L. (2015). microRNAs regulate β -catenin of the Wnt signaling pathway in early sea urchin development. *Developmental Biology*, *402*(1), 127-141. doi:<https://doi.org/10.1016/j.ydbio.2015.01.008>

- Stepicheva, N. A., & Song, J. L. (2014). High throughput microinjections of sea urchin zygotes. *J Vis Exp*(83), e50841. doi:10.3791/50841
- Stepicheva, N. A., & Song, J. L. (2015). microRNA-31 modulates skeletal patterning in the sea urchin embryo. *Development*, 142(21), 3769-3780. doi:10.1242/dev.127969
- Toch, M., Harris, A., Schakman, O., Kondratskaya, E., Boulland, J. L., Dauguet, N., . . . Clotman, F. (2020). Onecut-dependent Nkx6.2 transcription factor expression is required for proper formation and activity of spinal locomotor circuits. *Sci Rep*, 10(1), 996. doi:10.1038/s41598-020-57945-4
- Torii, K. U. (2012). Two-dimensional spatial patterning in developmental systems. *Trends Cell Biol*, 22(8), 438-446. doi:10.1016/j.tcb.2012.06.002
- Truman, J. W., Moats, W., Altman, J., Marin, E. C., & Williams, D. W. (2010). Role of Notch signaling in establishing the hemilineages of secondary neurons in *Drosophila melanogaster*. *Development*, 137(1), 53-61. doi:10.1242/dev.041749
- Tutukova, S., Tarabykin, V., & Hernandez-Miranda, L. R. (2021). The Role of Neurod Genes in Brain Development, Function, and Disease. *Front Mol Neurosci*, 14, 662774. doi:10.3389/fnmol.2021.662774
- van der Raadt, J., van Gestel, S. H. C., Nadif Kasri, N., & Albers, C. A. (2019). ONECUT transcription factors induce neuronal characteristics and remodel chromatin accessibility. *Nucleic Acids Res*, 47(11), 5587-5602. doi:10.1093/nar/gkz273
- Vega Thurber, R., & Epel, D. (2007). Apoptosis in early development of the sea urchin, *Strongylocentrotus purpuratus*. *Developmental Biology*, 303(1), 336-346. doi:<https://doi.org/10.1016/j.ydbio.2006.11.018>
- Wada, Y., Mogami, Y., & Baba, S. (1997). Modification of ciliary beating in sea urchin larvae induced by neurotransmitters: beat-plane rotation and control of frequency fluctuation. *The Journal of Experimental Biology*, 200(1), 9. Retrieved from <http://jeb.biologists.org/content/200/1/9.abstract>
- Wang, F., Tidei, J. J., Polich, E. D., Gao, Y., Zhao, H., Perrone-Bizzozero, N. I., . . . Zhao, X. (2015). Positive feedback between RNA-binding protein HuD and transcription factor SATB1 promotes neurogenesis. *Proc Natl Acad Sci U S A*, 112(36), E4995-5004. doi:10.1073/pnas.1513780112
- Wei, Z., Angerer, L. M., & Angerer, R. C. (2016). Neurogenic gene regulatory pathways in the sea urchin embryo. *Development*, 143(2), 298. doi:10.1242/dev.125989
- Wei, Z., Angerer, R. C., & Angerer, L. M. (2011). Direct development of neurons within foregut endoderm of sea urchin embryos. *Proceedings of the National Academy of Sciences of the United States of America*, 108(22), 9143-9147. doi:10.1073/pnas.1018513108
- Weng, R., & Cohen, S. M. (2012). *Drosophila* miR-124 regulates neuroblast proliferation through its target anachronism. *Development*, 139(8), 1427-1434. doi:10.1242/dev.075143
- Wessel, G. M., & McClay, D. R. (1985). Sequential expression of germ-layer specific molecules in the sea urchin embryo. *Developmental biology*, 111(2), 451-463. Retrieved from http://www.ncbi.nlm.nih.gov/entrez/query.fcgi?cmd=Retrieve&db=PubMed&dopt=Citation&list_uids=2412914

- Wessel, G. M., & Wikramanayake, A. (1999). How to grow a gut: ontogeny of the endoderm in the sea urchin embryo. *BioEssays : news and reviews in molecular, cellular and developmental biology*, 21(6), 459-471. Retrieved from http://www.ncbi.nlm.nih.gov/entrez/query.fcgi?cmd=Retrieve&db=PubMed&dopt=Citation&list_uids=10402953
- Yaguchi, J., Angerer, L. M., Inaba, K., & Yaguchi, S. (2012). Zinc finger homeobox is required for the differentiation of serotonergic neurons in the sea urchin embryo. *Developmental biology*, 363(1), 74-83. doi:10.1016/j.ydbio.2011.12.024
- Yaguchi, J., Takeda, N., Inaba, K., & Yaguchi, S. (2016). Cooperative Wnt-Nodal Signals Regulate the Patterning of Anterior Neuroectoderm. *PLoS Genet*, 12(4), e1006001. doi:10.1371/journal.pgen.1006001
- Yaguchi, J., & Yaguchi, S. (2021). Sea urchin larvae utilize light for regulating the pyloric opening. *BMC Biology*, 19(1), 64. doi:10.1186/s12915-021-00999-1
- Yaguchi, S., & Katow, H. (2003). Expression of tryptophan 5-hydroxylase gene during sea urchin neurogenesis and role of serotonergic nervous system in larval behavior. *The Journal of comparative neurology*, 466(2), 219-229. doi:10.1002/cne.10865
- Yaguchi, S., Yaguchi, J., Angerer, R. C., & Angerer, L. M. (2008). A Wnt-FoxQ2-nodal pathway links primary and secondary axis specification in sea urchin embryos. *Developmental cell*, 14(1), 97-107. doi:S1534-5807(07)00390-5 [pii]10.1016/j.devcel.2007.10.012
- Yaguchi, S., Yaguchi, J., Angerer, R. C., Angerer, L. M., & Burke, R. D. (2010). TGF β signaling positions the ciliary band and patterns neurons in the sea urchin embryo. *Developmental biology*, 347(1), 71-81. doi:10.1016/j.ydbio.2010.08.009
- Yaguchi, S., Yaguchi, J., & Burke, R. D. (2006). Specification of ectoderm restricts the size of the animal plate and patterns neurogenesis in sea urchin embryos. *Development*, 133(12), 2337-2346. doi:10.1242/dev.02396
- Yaguchi, S., Yaguchi, J., Wei, Z., Jin, Y., Angerer, L. M., & Inaba, K. (2011). Fez function is required to maintain the size of the animal plate in the sea urchin embryo. *Development*, 138(19), 4233. doi:10.1242/dev.069856
- Yamazaki, A., Kawabata, R., Shiomi, K., Tsuchimoto, J., Kiyomoto, M., Amemiya, S., & Yamaguchi, M. (2008). Kruppel-like is required for nonskeletogenic mesoderm specification in the sea urchin embryo. *Dev Biol*, 314(2), 433-442. doi:10.1016/j.ydbio.2007.11.035
- Yoshihiro, M., Keiko, W., Chieko, O., Akemi, K., & Baba, S. A. (1992). Regulation of ciliary movement in sea urchin embryos: Dopamine and 5-HT change the swimming behaviour. *Comparative Biochemistry and Physiology Part C: Comparative Pharmacology*, 101(2), 251-254. doi:[https://doi.org/10.1016/0742-8413\(92\)90269-D](https://doi.org/10.1016/0742-8413(92)90269-D)
- Yu, J. Y., Chung, K. H., Deo, M., Thompson, R. C., & Turner, D. L. (2008). MicroRNA miR-124 regulates neurite outgrowth during neuronal differentiation. *Experimental cell research*, 314(14), 2618-2633. doi:10.1016/j.yexcr.2008.06.002
- Zaharieva, E., Haussmann, I. U., Brauer, U., & Soller, M. (2015). Concentration and Localization of Coexpressed ELAV/Hu Proteins Control Specificity of mRNA

Processing. *Molecular and cellular biology*, 35(18), 3104-3115.
doi:10.1128/MCB.00473-15

Figure legends

Figure 1. NeuroD1 regulates transcripts involved in the neuronal GRN. (A) Three neuronal domains are specified during the blastula stage. Neuronal progenitors will differentiate and mature into functional neurons in the larvae stage. AD=apical domain, MF=mouth formation, CB=ciliary band, EM=endomesoderm. AO=apical organ, CBN=ciliary band neurons, EMN=endomesodermal neurons. (B) Physiological embryos were collected (Egg (0 hpf), morula (14 hpf), blastula (24 hpf), gastrula (48 hpf), larval (72 hpf), and five days post fertilization (120 hpf). Three biological replicates. (C) Control MASO or *NeuroD1* MASO-injected embryos were collected for qPCR at gastrula and larval stages. Transcripts of genes that encode factors involved in neuronal development are examined. Four biological replicates. Purple=neuron-restricted progenitor gene marker, blue=post-mitotic neuronal gene marker, grey=mature neuronal gene marker, yellow=mature and functional neuronal

gene marker, white=ciliary band gene marker. (D) Control MASO or *NeuroD1* MASO-injected larvae were immunolabeled with SynB (green) and counterstained with DAPI. Three biological replicates.

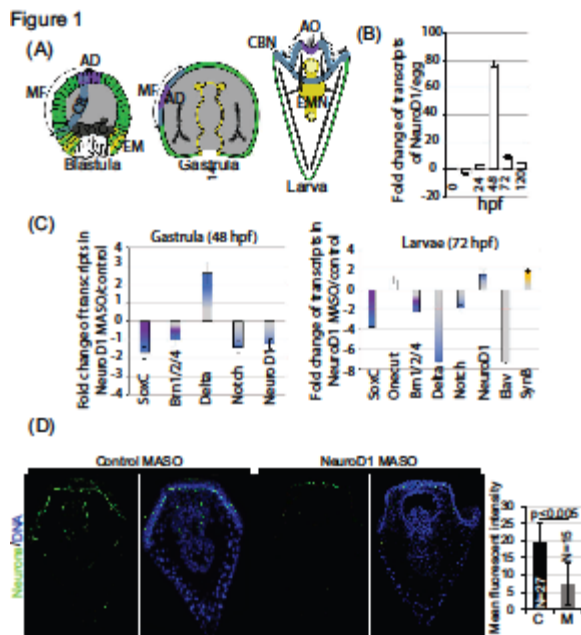


Figure 2. miR-124 is enriched in ciliary band. (A) Embryos were hybridized with miR-124 probe or a scrambled control probe (green) using FISH. Three biological replicates. (B) Double FISH was performed with DIG-labeled miR-124 probe (green) and fluorescein-labeled *Onecut* (magenta) and counterstained with DAPI to visualize DNA (blue). miR-124 is expressed in basal side of epithelial cells (white arrow), where neurons reside, juxtaposed to epithelial cells that express *Onecut* expression on the apical side (yellow arrow). Two biological replicates.

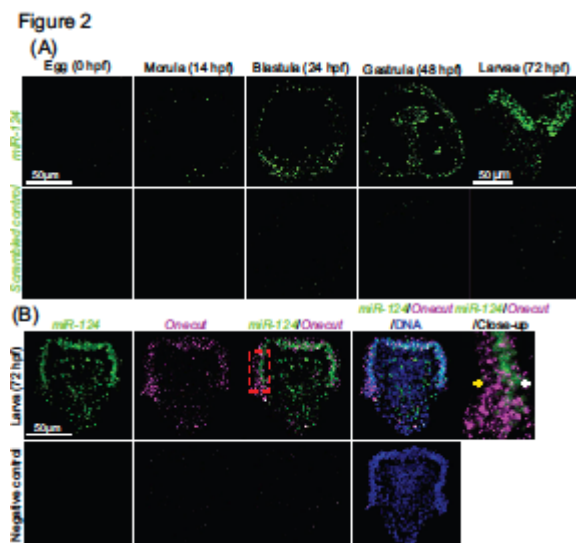


Figure 3. Inhibition of miR-124 leads to endodermal and mesodermal developmental defects. (A) miR-124 inhibitor or control were injected into zygotes and cultured to blastulae (24 hpf), followed by miR-124 FISH (green). Embryos were counterstained with DAPI (blue). Average fluorescence intensity was calculated. Student t-test was used. Three biological replicates. (B) Developmental defects in miR-124 inhibitor-injected embryos are indicated by the white arrows. Cochran-Mantel-Haenszel statistical test was used. Four biological replicates. For all the graphs, C=Control, Inh=miR-124 inhibitor-injected embryos, N= total number of embryos, SEM is graphed.

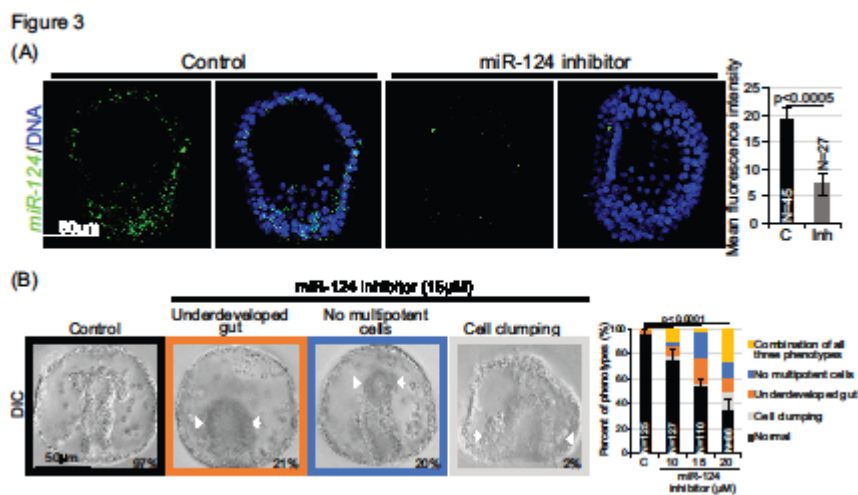
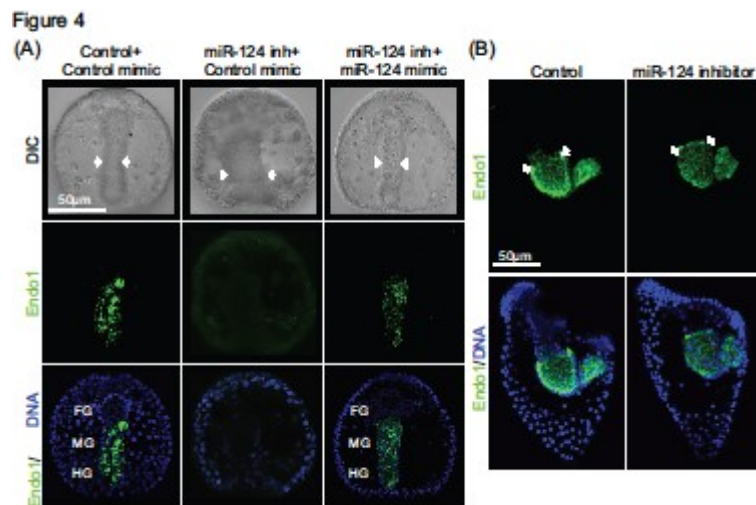


Figure 4. miR-124 inhibition leads to gut and sphincter defects. (A) miR-124 inhibitor-injected gastrulae were collected at 48 hpf and immunolabeled with Endo1 (green) and counterstained with DAPI (blue). Control N=12, miR-124 inhibitor-injected embryos N=10, and miR-124 inhibitor+miR-124 mimic N=7. White arrows point to the width of the midgut. (B) Larvae were immunolabeled with Endo1 and counterstained with DAPI. N=10 for both control and inhibitor. (C) Gut contractions were counted from living larvae. (D) Phalloidin stain (green) indicated that miR-124 inhibitor-injected larvae had a wider cardiac sphincter. White arrows delineate the width of the cardiac sphincter. Three biological replicates for all experiments. For all the images, FG=Foregut, MG=Midgut, and HG=Hindgut.



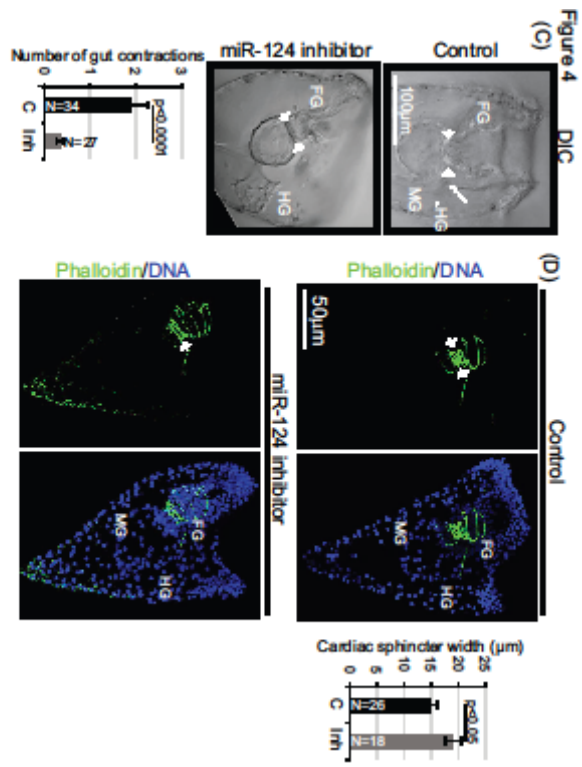


Figure 5. miR-124 inhibition results in decreased larval swimming velocity. (A) miR-124 inhibitor-injected embryos exhibited a significant decrease in swimming velocity. These defects were rescued with a co-injection of miR-124 inhibitor and miR-124 mimic. Three biological replicates. (B) Embryos were imaged live to assess cilia beating for 120 sec with polybeads. Three biological replicates. (C) Control and miR-124 inhibitor-injected embryos were immunolabeled with tubulin antibody (green) and counterstained with DAPI (blue). Three biological replicates. (D) miR-124 inhibitor-injected larvae exhibited a decrease in *Onecut* (green) expression and counterstained with DAPI. Four biological replicates. Control=51 and miR-124 inhibitor=52. For all the graphs, C=Control, Inh=miR-124 inhibitor-injected embryos, N= total number of embryos.

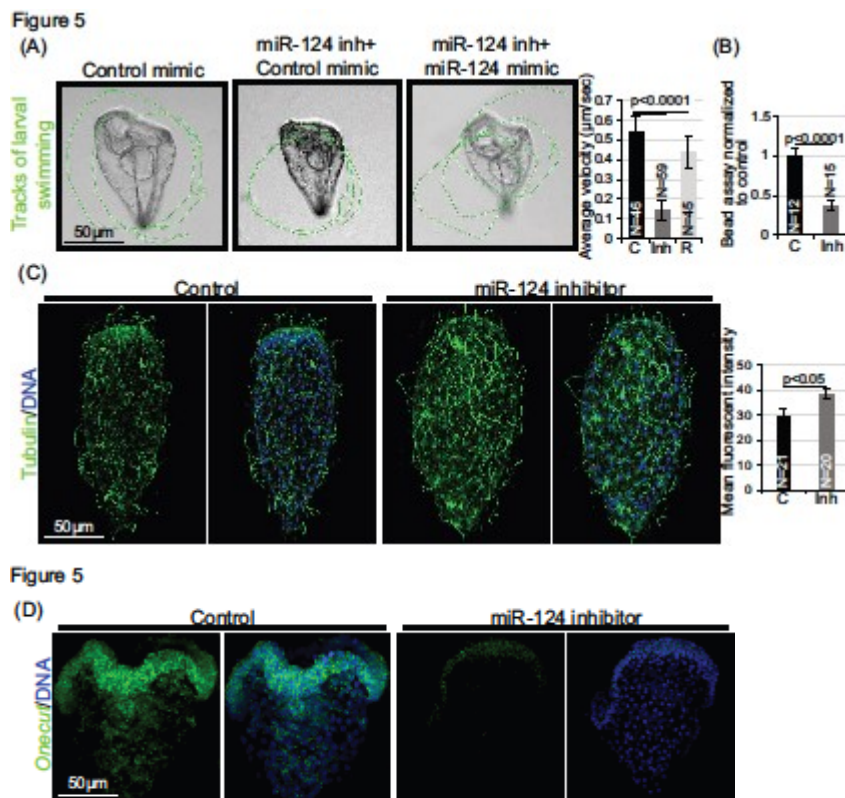


Figure 6. miR-124 regulates neurogenesis. (A) Oral view of serotonin-containing neurons (magenta) with a close-up view (shown by the inset delineated by the white dashed lines) and counterstained with DAPI (blue). The arrows indicate dendritic spines. (B) miR-124 inhibitor-injected larvae were immunolabeled with sea urchin neuronal antibody 1E11 that detects SynB-expressing neurons (green) and counterstained with DAPI. Co-injection of miR-124 inhibitor with miR-124 mimic

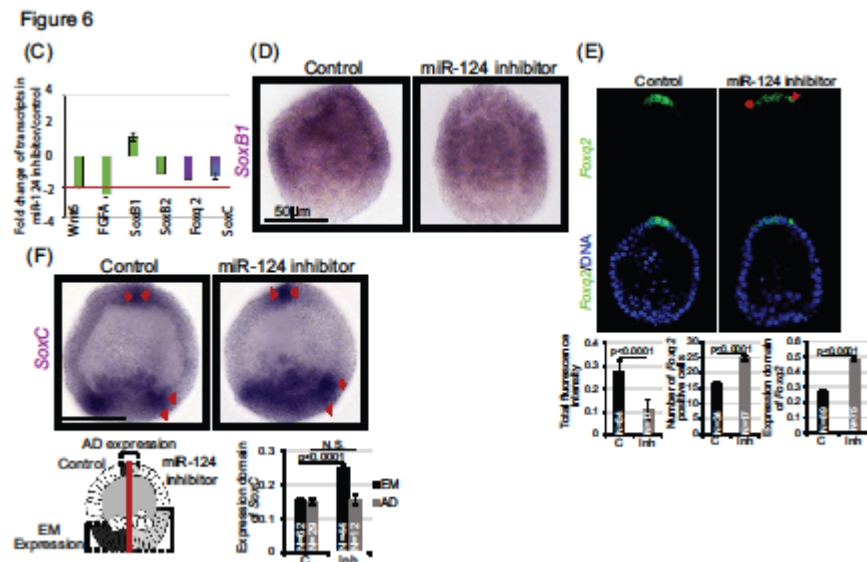
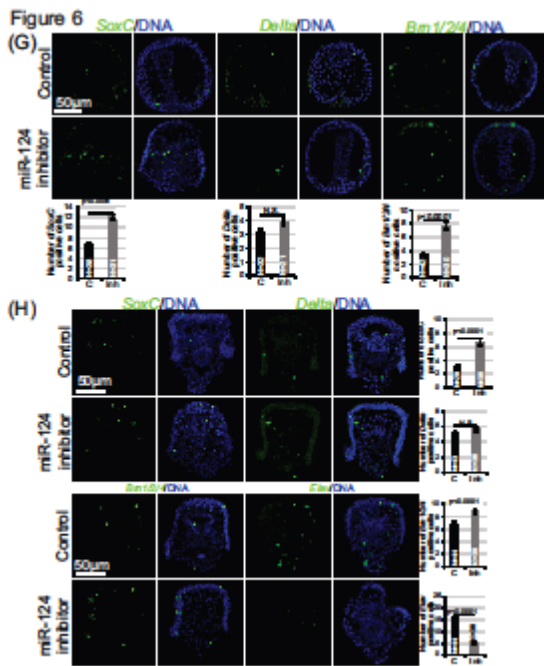


Figure 7. miR-124 directly suppresses *NeuroD1* to regulate gut contractions and swimming. (A) Dual-luciferase assays indicated that miR-124 directly suppresses *Notch* at binding site seed 1 (S1) and *NeuroD1* seed. Each biological replicate contained 25 embryos. (B) Blocking miR-124's suppression of *NeuroD1* using *NeuroD1* TP resulted in decreased but not significant gut contractions. Representative images of gut contractions are depicted. FG=foregut, MG=midgut, HG=hindgut. (C) Larvae were imaged live to obtain the swimming velocity. (D) Embryos were imaged live for cilia beating. (E) *NeuroD1* TP-injected larvae exhibited an increase in tubulin (green). Larvae were counterstained with DAPI (blue). Three biological replicates for all experiments. CTP=Control Target Protector, NTP=*NeuroD1* Target Protector, N= total number of embryos.

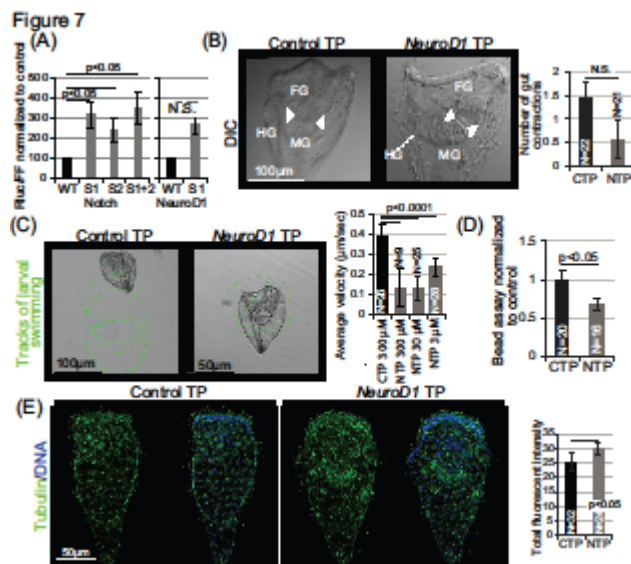


Figure 8. miR-124's direct regulation of *NeuroD1* is important for neurogenesis. (A) Oral view of serotonergic neurons (magenta) with a close-up view (shown by the inset delineated by the white dashed lines) and counterstained with DAPI (blue). (B) *NeuroD1* TP-injected larvae were immunolabeled with sea urchin neural antibody 1E11 (green) and counterstained with DAPI. (C) Relative levels of neuronal transcripts in control or *NeuroD1* TP-injected blastulae were measured with qPCR. Green=neural stem cell gene marker, purple=neuron-restricted progenitor gene marker, blue=post-mitotic neuronal gene marker. (D) *Foxq2* expression domains were similar in control and *NeuroD1* TP-injected blastulae. (E) Neuronal transcripts (green) in control and *NeuroD1* TP-injected gastrula embryos were assessed using FISH and counterstained with DAPI. (F)

Neuronal transcripts (green) in control and *NeuroD1* TP-injected larval embryos were assessed using FISH and counterstained with DAPI. Three biological replicates for all experiments. CTP=*Control Target Protector*, NTP=*NeuroD1 Target Protector*, N=total number of embryos.

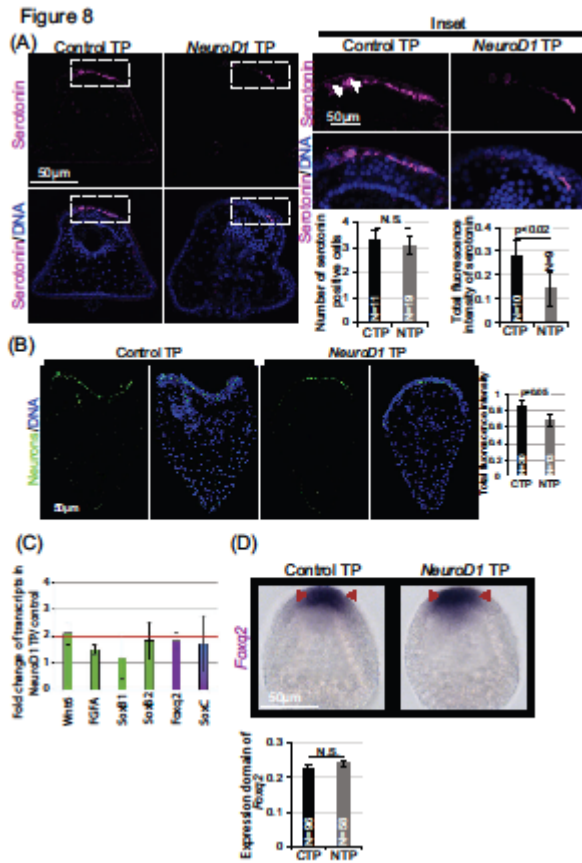


Figure 9. Removal of miR-124's inhibition of *Notch* and/or *NeuroD1* result in decreased mature neurons and increased apoptosis. (A) Control TP or *NeuroD1* TP and *Notch* TP were injected into zygotes and assessed for the number of *Elav*-expressing cells in the larvae. Co-injection of *NeuroD1* and *Notch* TPs recapitulated miR-124 inhibition in reducing mature neurons (*Elav*-expression). (B) To assess changes in apoptotic cells, we injected control TP or *Notch* TP into zygotes. We used TUNEL assay to assess cells undergoing apoptosis (green) and counterstained embryos with DAPI (blue). *Notch* TP-injected embryos undergo significantly increased apoptosis compared to the control. Three biological replicates for all experiments. N=total number of embryos.

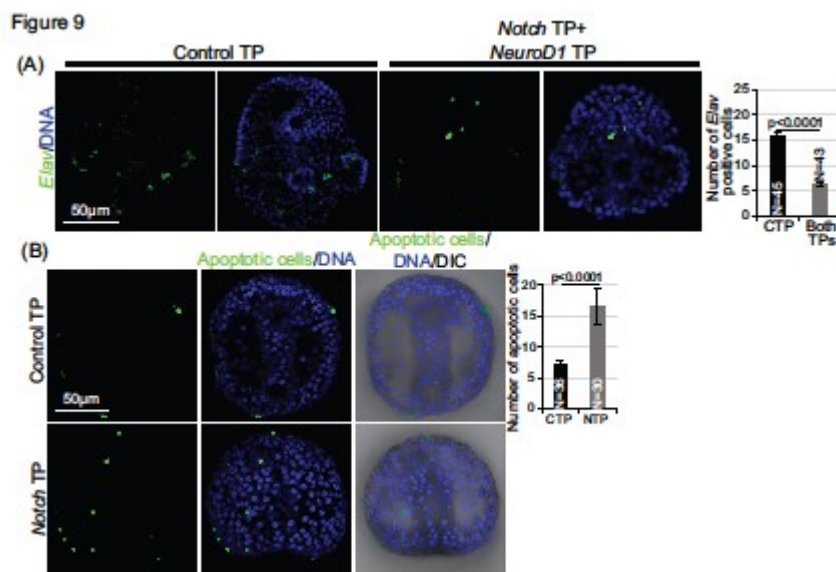


Figure 10. Working model of post-transcriptional control mediated by miR-124 in modulating neurogenesis. miR-124 regulates an unknown factor to regulate expression changes in *Wnt6*, *FGFA*, and *Foxq2* to mediate neuronal specification in the blastula stage. During the gastrula stage, miR-124 is likely to regulate an unidentified factor that regulates *SoxC* and *Brn1/2/4* to mediate neuronal differentiation. miR-124 directly suppresses *Notch* to regulate the balance of *Delta*-expressing cells to become differentiated. *NeuroD1* expression peaks during the gastrula stage to potentially influence *Delta*. Later during the larval stage, *NeuroD1* also influences *SoxC*, *Delta*, *Brn1/2/4*, and *Elav* transcript levels. miR-124 suppresses *NeuroD1* to modulate neuronal differentiation and maturation during the late gastrula and larval stages. Transcripts such as *SoxC*, *Delta*, and *Brn1/2/4* are also expressed in the endomesoderm in the blastula. Important to note is that gene expression of various factors depicted here is focused on cells of the neuronal lineage and does not include their expression in the endomesoderm. Green=neural stem cell gene marker, purple=neuron-restricted progenitor gene marker, blue=post-mitotic neuronal gene marker, grey=mature neuronal gene marker, yellow=mature, and functional neuronal gene marker. Made with Biorender.com.

Figure 10

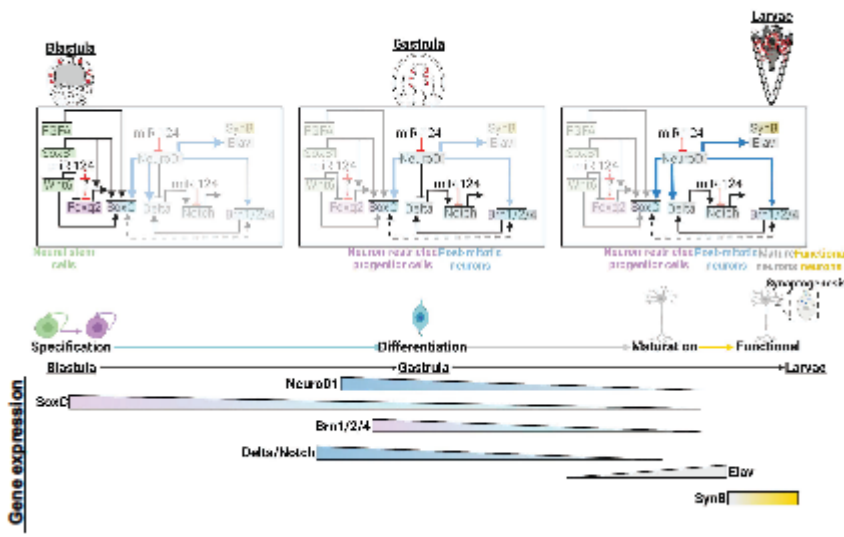


Table 1. List of primers and sequences of injections solutions					
Primers for whole mount <i>in situ</i> hybridization					
Gene s	Forward (5' to 3')	Reverse (5' to 3')	Ve cto r	Enz ym es	Poly mer ase
SoxB1	ACGAACCGGAGTTGAAG	ATTTAGGTGACACTATAGCAGC CTGTTGCATAGCATGT	Zer o- blu nt	Ba mH I	T7
Foxq2	GATTTAGGTGACACTATAGTTG AAAACCT	ATTTAGGTGACACTATAGTGCAT CGCTGGTGGTAGTAG	Zer o- blu nt	Ba mH I	T7
Onec ut (Hnf6)	GTTTGGAGGCATGTTGGAGT	ATTTAGGTGACACTATAGTTTGA GATCCGGCCATACAC	Zer o- blu nt	Xb al	Sp6
SoxC	GTTCTCAGAAGAGCTTCGC	ATTTAGGTGACACTATAGGTCG ACATGGACGATTGCT	Zer o- blu nt	Sac I	T7
Brn1/ 2/4	ATCAGAAATTGGGCAACGAG	ATTTAGGTGACACTATAGTGAAT CAGCGCTTTCATAC	Zer o- blu nt	Ba mH I	T7
Elav	GCTAACAGGCCAATCTCTGG	ATTTAGGTGACACTATAGAGCT CGTCATGGGATTGAAC	Zer o- blu nt	Ap al	Sp6
Delta	TGGATGCGACTTTTGTATGC	ATTTAGGTGACACTATAGTGCA AGCCTTCTGTGGATG	Zer o- blu nt	Sac I	T7
Primers for cloning areas of the genes that contain the seed sites					
Gene s	Forward (5' to 3')	Reverse (5' to 3')	Ve cto r		
Notch	AAGCTTAAAACAAACAAACATG CTTATTG	GCGGCCGCGACTTTCAGGGG CATTCT	RL UC	Eco RI	Sp6
Neuro	CTCGAGCAAGTACAGTCCAGCC	GCGGCCGCCCGCGGTATAAAT	RL	Eco	Sp6

D1	GACA	CTTGTCC	UC	RI	
Primers for Quickchange mutagenesis					
Gene	Forward (5' to 3')	Reverse (5' to 3')	Vector		
Notch first seed in 3'UTR	ACCTTAATCCCTCGAGAACAAT GCGCAATTTGATAATTTACACAT AAAAGTTTC	GAAACTTTTATGTGTAAATTATC AAATTGCGCATTGTTCTCGAGG GATTAAGGT	RL UC		
Notch second seed in 3'UTR	TACAAGGTATATTGGCAGTGAA TGCGCGTTTGAAAGTTTTTCAGT TTGC	GCAAACCTGAAAACCTTTCAAACG CGCATTCACTGCCAATATACCTT GTA	RL UC		
Neuro D1 1 seed in CDS (seed deleted)	GCACTGCTTGGCTGTACGGTGA CGTCTG	CAGACGTCACCGTACAGCCAAG CAGTGC	RL UC		
Primers for injecting transcripts					
Gene	Forward (5' to 3')	Reverse (5' to 3')	Vector	Enzymes	Polymerase
Neuro D1	CTCGAGCAAGTACAGTCCAGCC GACA	ATTTAGGTGACACTATAGCCGC GGTATAAATCTTGTCC	Zer o- Blu nt	Sac I	T7
Primers for qPCR					
Gene	Forward (5' to 3')	Reverse (5' to 3')			
Ubiquitin	CACAGGCCAAGACCATCACAC	GAGAGAGTGCGACCATCCTC			
Wnt6	AGACATCTGCCTCCGTGAAC	ATGATGCCTCAGCTGGAAC			
Foxq2	TCTCTCCCTCAACGAGTGCT	TCTTCAAGGTTAGCGGGATG			

SoxB 2	GAAGGAGCATCCCCACTACA	GAATACAGGGGATCGGGAAT			
SoxB 1	TGTGAACGTCATGGCAAGTT	GGGTTGCTGTTGTTCTTGT			
Brn1/ 2/4	GCTAACAGGCCAATCTCTGG	CATTGAAGACGCAATCCATTT			
Neuro D1	CGGACTGAATGATGCACTTG	TTCTTTGCGAGGCGTAGAGT			
SoxC	GTACGTCGAGGAGGCAGAGA	TGGCTTAGTGGTAGGCTTGG			
FGFA	CTTGGGAGAGAGGGAAAAGG	GTGTCGTGAATGACAGACGTG			
Synap totag min B (SynB)	CCCAGTTCCAACCTCCTG	AGTGAAGAAGAGATCGGCCA			
Elav	TGATGAGGACAGCAAGACCA	TGACCAGTTTGCAGGATTCA			
Delta	ACGGAGCTACATGCCTGAAC	TCACAATGGACCGAATCAGA			
Notch	ACGGAGCCAAGCCTAAGAA	TCGTCACAGGCAACGAATAA			
Onec ut (Hnf6)	CAAGAACCCGAGTTCCAGAG	TCTTGATGTGGCTGTTCTGC			
Primers for cloning into protein expression vector					
Gene	Forward (5' to 3')	Reverse (5' to 3')	Ve cto r		
Neuro D1 in pNoT AT	GGTACCATGGGCCCCACCCTA CATGA	CTCGAGTTAACCGCGGTATAAA TCTTGTC	pN oT AT		
Sequences of MASOs					
Gene	Sequence				
Neuro D1 MAS O	AGTTCCTTTTTTATGACGTT				
Neuro D1	GGCCAGGCACTGTACGGTGAT GTCT				

miR-124 TP					
Neuro D1 contro I TP #1	TCGGCGCTCGACGTCAGGCAA GATG				
Neuro D1 contro I TP #2	CCATCGCTGCATTAAGACCATA GTG				
Notch miR-124 TP	GAACAAGGCACAATTTTCATAATT TA				
Notch contro I TP #1	CCCGACAGCTACGTCGTGTACT GGA				
Notch contro I TP #2	ATGCACATTATCAATGCACATAC AT				
Sequences of LNAs					
Name	Sequence				
HSA-miR-124-3P miRC URY LNA miRN A Detec tion Probe	GGCATTACCCGCGTGCCTTA				
Scra mble-miR miRC URY	GTGTAACACGTCTATACGCCCA				

LNA Detec tion probe, negati ve contro l					
HSA- miR- 124- 3P miRC URY LNA miRN A Power Inhibit or	GCATTCACCGCGTGCCTTA				
HAS- miR- 124- 3P miRC URY LNA miRN A Mimic	UAAGGCACGCGGUGAAUGCC				
Negat ive Contr ol miRC URY LNA miRN A Mimic	UCACCGGGUGUAAAUCAGCUU G				

miR-124 seed in red

KpnI restriction site in green

XhoI restriction site in blue